AD-A093 927 NEVADA UNIV RENO DESERT RESEARCH INST F/G 4/2
CHARACTERISTICS OF ATMOSPHERIC ICE PARTICLES: A SURVEY OF TECHN--ETC(U)
SEP 80 J HALLETT F19628-80-C-0054
UNCLASSIFIED AFGL-TR-80-030A NL

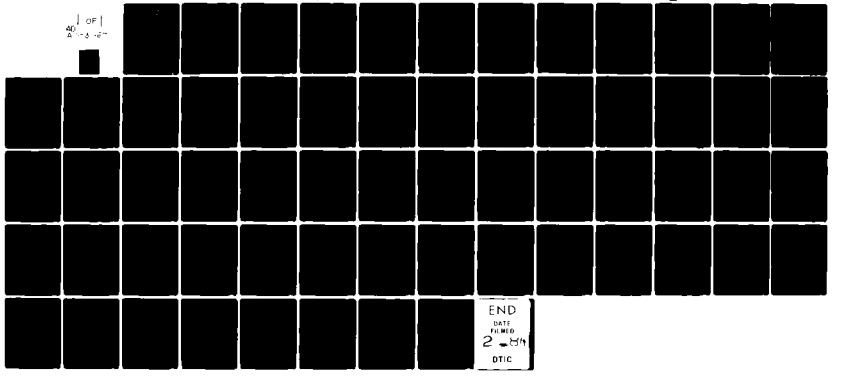

AFGL-TR-80-0308

LEVEL II

(12)

CHARACTERISTICS OF ATMOSPHERIC ICE PARTICLES: A SURVEY OF TECHNIQUES

John Hallett

University of Nevada System
Desert Research Institute
Reno, Nevada 89506

Final Report
January through September 1980

September 1980

Approved for public release; distribution unlimited

AIR FORCE GEOPHYSICS LABORATORY
AIR FORCE SYSTEMS COMMAND
UNITED STATES AIR FORCE
HANSCOM AFB, MASSACHUSETTS 01731

Unclassified

SECURITY CLASSIFICATION OF THIS PAGE (When Data Entered)

(19) REPORT DOCUMENTATION PAGE	READ INSTRUCTIONS BEFORE COMPLETING FORM
1. REPORT NUMBER (18) AFGL-TR-80-0308	2. GOVT ACCESSION NO. AD-A093 927
4. TITLE (and Subtitle) (6) CHARACTERISTICS OF ATMOSPHERIC ICE PARTICLES: A SURVEY OF TECHNIQUES,	5. TYPE OF REPORT & PERIOD COVERED (9) Final Report, January - September 1980,
	6. PERFORMING ORG. REPORT NUMBER
7. AUTHOR(s) (10) John Hallett	8. CONTRACT OR GRANT NUMBER(s) (15) F19628-80-C-0054
9. PERFORMING ORGANIZATION NAME AND ADDRESS University of Nevada Desert Research Institute Reno, Nevada 89507 (12) (16)	10. PROGRAM ELEMENT, PROJECT, TASK AREA & WORK UNIT NUMBERS 61102F 2310G5AF (17)
11. CONTROLLING OFFICE NAME AND ADDRESS Air Force Geophysics Laboratory Hanscom AFB, Massachusetts 07131 Tech nical Monitor/Don McLeod/LYC (11)	12. REPORT DATE September 1980
	13. NUMBER OF PAGES 54
14. MONITORING AGENCY NAME & ADDRESS(if different from Controlling Office)	15. SECURITY CLASS. (of this report) Unclassified
	15a. DECLASSIFICATION/DOWNGRADING SCHEDULE

16. DISTRIBUTION STATEMENT (of this Report)

Approved for public release; distribution unlimited

17. DISTRIBUTION STATEMENT (of the abstract entered in Block 20, if different from Report)

18. SUPPLEMENTARY NOTES

19. KEY WORDS (Continue on reverse side if necessary and identify by block number)

Cloud physics
Cirrus crystals
Ice crystals
Ice crystal mass
Instrumentation
Ice measurement

20. ABSTRACT (Continue on reverse side if necessary and identify by block number)

A survey is given of properties of ice particles in the atmosphere necessary to assess the design of aircraft instrumentation required for their characterization. A critical review is given of current aircraft instrumentation from the view point of representative data acquistion in a realistic time frame, in particular techniques for mass and size distribution are examined. It is concluded that two as yet untried techniques utilizing particle accretion and evaporation show promise for measurement of mass distribution.

DD FORM 1 JAN 73 1473 EDITION OF 1 NOV 65 IS OBSOLETE

Unclassified

SECURITY CLASSIFICATION OF THIS PAGE When Data Entered

20.

TABLE OF CONTENTS

TABLE OF CONTENTS

(continued)

LIST OF FIGURES

PERSONNEL

Principal Investigator - John Hallett

Associate Investigators - Dr. V. N. Smiley (Optical Technology)

Dr. W. Gaskell (Contact charging)

R. Purcell (Mechanical techniques)

INTRODUCTION: Ice particles in the atmosphere

Ice particles found in the atmosphere result from growth by vapor deposition or droplet accretion, or a combination of these two processes, over a period often in excess of one thousand seconds. The initial ice may be nucleated in several ways - directly on a deposition nucleus, by a freezing nucleus contained in a supercooled cloud droplet or rain drop or by contact at a droplet surface following Brownian capture. Subsequent growth of these initial particles produce varying characteristics depending on the ambient conditions - temperature, supersaturation, size of accreted droplets, and the terminal fall velocity of the particle. The particle itself may be essentially two dimensional - as a hexagonal plate or dendrite growing from a central nucleus - such that material is added at the periphery alone. In contrast some particles are conical, with drops being added only at the base of the cone; on the other hand some particles tumble, in which case droplets are accreted nearly symmetrically to produce an approximately spherical shape. This latter situation gives rise to an onion ring structure typical of the layers seen in larger hail stones. In each case, the particular accretion and vapor growth geometry gives a structure which depends on the history of the growth conditions and varies outwards from the site of the initial particle to the growth perimeter. This variation is most commonly manifest in terms of density, with greater or less volume of included air trapped between individual crystals or accreted drops, or, in the case of hail stones, rejected from the liquid during growth. Physical properties, such as fracture strength and crystal texture (individual crystal size and orientation) depend on the growth conditions and change with the position in the particle in a similar manner.

These considerations show that prediction of ice particle characteristics require an intimate knowledge of conditions throughout its growth history, which in practice is quite unrealistic. It is therefore necessary to make empirical measurements of the ice particle characteristics in order to make some overall classification with more general meteorological conditions. An alternative approach is to grow the particles under laboratory simulation. This latter technique has met with some success in assessing characteristics, such as habit and graupel density, but has not been so successful in giving information on the more complex vapor or accretion growth of particles occurring in the dynamical, time-dependent framework of a real cloud.

In the first part of this report, a survey is given of the important properties of ice particles, obtained from both field and laboratory studies, which is relevant to the application in a meteorological context, and also relevant to the development and utilization of instruments to obtain ice particle information on a more extended scale in the atmosphere. The complex formative and metamorphic processes which give rise to the wide range of particle properties require a wide dynamic range of instrumentation for characterization. Under some situations suitable instrumentation from the operational view point is not available (Barnes 1978). The second part of this report examines instrumentation currently available together with new possible techniques for particle characterization.

PART I: ICE PARTICLE CHARACTERIZATION

From the viewpoint of all applications a knowledge of ice particle concentration is a prerequisite. Size and shape are of prime interest from the optical viewpoint, whereas mass is of prime interest from the viewpoint of vehicle interaction. For hydrological studies, precipitation rate and a knowledge of particle fall velocity in addition to mass is required.

In practice, direct photography, replication and electro-optical shadow probes, give a knowledge of projected area. The third dimension can be inferred from known ice particle characteristic and the statistics of the particle orientation during measurement. Density may be obtained from direct atmospheric measurement, that is size and mass, and similarly from laboratory simulation studies. Particle mass can be inferred from a particle dimension with a knowledge of its shape and the mean density. Obtaining these quantities in a systematic way and automating acquisition of the data has proved a difficult undertaking; the limitations of current technology and the basic physical reasons for their limitations is the subject of this report.

Particle Concentrations

Typical measured concentration of ice crystals in the atmosphere show highest values for smaller size (Fig. 1). This relation follows in part from the competitive nature of particle nucleation and growth. For example, small particles found in cold ($< -40^{o}C$) lenticular clouds or ice fogs, result from

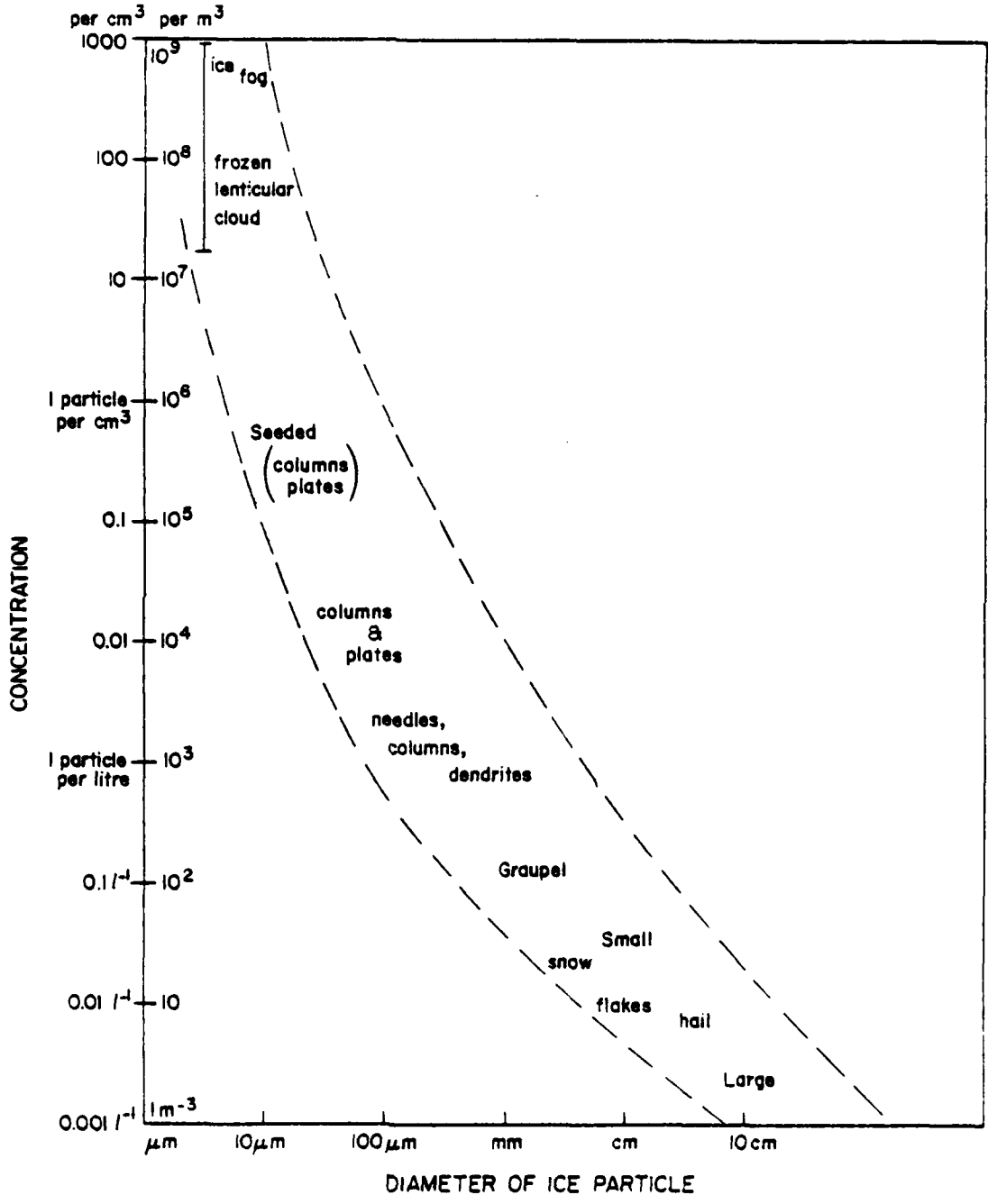

Fig 1 Typical size and concentration of atmospheric ice particles.

solution droplets formed on hygroscopic cloud condensation nuclei, which dilute to larger cloud droplets and subsequently freeze. Larger ice particles of lower concentration result from growth at higher temperature of particles formed by heterogeneous nucleation, that is by impurity particles, which give a somewhat arbitrary, but lower concentration of ice particles, which, at these higher temperatures, grow in the absence of any mutual competition with neighbors. In general, more particles nucleate at lower temperatures until -40°C is reached, according to:

$$N(T_s) = N_o e^{a T_s} \quad \text{where } T_s = \text{temperature below } 0^\circ\text{C}$$

and a is constant.

Alternatively, ice particle concentrations may result from the input of ice particles nucleated at temperatures below -40°C, which have fallen out or been advected downwards, a fraction of which grow to larger size in competition with their neighbors for the available vapor. This is the snowfall situation fed by ice crystals from a cloud aloft. Somewhat similarly, the highest concentration of graupel particles occurs with nucleation of supercooled drops in convective cloud consistent with no competition for the available cloud drops. In general, the concentration of particles is substantially less than the upper competitive limits, as ice particle concentration is limited by the available nuclei. This is in contrast to the case where secondary ice crystal formation occurs when the whole cloud can be transformed to ice.

A further question to be considered is the extent of the spread of particle sizes present at any one position in the cloud and the physical processes responsible for this spread. An in situ process which gives a spread of particles in quite a distinct way occurs with secondary ice production. This gives graupel (mm) and vapor grown ice columns (100 to 200 μm) coexisting in regions lying somewhat above the -3°C to -8°C level, where the vapor grown columns have had time (at least 100 s) to grow (Hallett et al., 1978).

It is pointed out that sedimentation in a rapidly rising, cooling air parcel does <u>not</u> necessarily produce a substantial spread of sizes. Successive nucleation in an ascending cooling updraft produces particles which fall into air containing smaller particles below, only as the updraft weakens; a similar process is operative in convective elements giving rise to cirrus unicus. Sedimentation of horizontally

advected particles gives rise to more pronounced bimodal spectra (as in the secondary ice production case) although this process is only active in specific situations, as for example, when ice formed in an old decaying cloud tower is ingested by a new rising tower (Keller and Sax 1981).

With the bimodal and wide ice particle size spectrum, instrument criteria are more rigid than otherwise; simultaneous measurement of 100μm columns and 1 mm graupel require a tenfold size discrimination and a 1000 fold mass discrimination; this underlines the nature of the problem.

Particle Shape

Ice crystals growing from the vapor may begin on frozen drops or on solid insoluble particles. Cloud and rain drops nucleating at smaller supercooling have a greater likelihood of being single crystals, smaller drops being monocrystalline to larger supercooling (Hallett, 1963). In these cases, vapor growth leads to forms with a single crystallographic orientation. This growth is specified by the crystal habit (ratio of "c" to "a" direction growth) and the extent of skeletal growth, that is the departure from growth as basal or prism plane facets. This gives dendrites or sector plates with preferred growth in the "a" axis direction, at the tips of the hexagon; alternatively, as needles or hollow columns, with preferred growth in the "c" axis direction from the hexagon corners or the complete hexagon periphery respectively. Laboratory and field studies have shown that such growth depends crucially on the environmental temperature, the environmental supersaturation and the ventilation velocity of the crystal as it falls (Table 1) (Kobayashi, 1957, 1965; Hallett and Mason, 1958; Keller and Hallett, 1981).

Near water saturation it appears that crystalline defects are unimportant in determining crystal habit, which is related only to temperature with three transitions at $-3^{o}C$, $-8^{o}C$ and $-25^{o}C$; the habit changes are related to specific temperature dependent properties for nucleation on molecularly smooth crystal facets. At smaller supersaturation, on the other hand, at $<$ 0.5 ice-water saturation at temperatures above $-18^{o}C$, (McKnight and Hallett, 1978) there does appear to be evidence from x-ray topographic studies that defects are responsible for growth. In this case, the possibility exists that habits other than those found at water saturation could occur, giving shapes not normally expected in a particular temperature regime. This is more likely to happen for smaller ($<$100 μm) crystals, with small fall velocity, since enhanced fall velocity of the large crystals gives an effective higher supersaturation at the crystal tips, which

TABLE I

ICE CRYSTAL HABIT AND SKELETAL STRUCTURE

Temperature °C	Very low supersaturation*	"Low" supersaturation+	"High" supersaturation or high ventilation velocities++
0 to -2	plates	plates	plates
-2 to -3	disc, plates	plates	dendrites
-3 to -8	disc, plates	hollow column	hollow column
-4 to -5	disc, plates	hollow column	needles
-8 to -12	disc, plates	plates	plates
-12 to -18	plates	plates	dendrites
-18 to -25	?	plates	plates
$< -25^{\circ}C$	column, plates; "a", "c" axes ice sheet	hollow column	needles

Plates and dendrites grow faster in the prism plane direction with a/c ratio $\lesssim 100$; columns and needles grow faster in the basal plane direction with a/c $\lesssim .01$.

*Very low supersaturation - $\sim 1/10$. (ice-water saturation) plate habit grows when nucleated on surfaces, with discs as initial growth form. Plate or column habit possible in preferred defect controlled growth.

+ 2/10 to 5/10 ice-water saturation in still air, or for small crystals (<200 μm) at terminal velocity.

++ 5/10 to 1.0 ice-water saturation or at lower (2/10 to 5/10 ice-water) supersaturation under forced ventilation and at higher terminal velocity for large (mm) crystals.

obviates the necessity for defects in growth (Keller, McKnight and Hallett, 1980). A further complexity may arise with the growth of individual crystals, thickness $\sim$50 μm in one "a" axis direction but extensive in one "a" axis and the "c" axis direction. These have been observed at the surface by Kikuchi (1970, 1971) and in the laboratory by Yamashita (1971) and Keller and Hallett (1981). These crystals have an external shape which can vary from rectangular to triangular and may contain ribs. Laboratory studies show that they are most likely to occur at temperatures $\sim -30^{o}C$ and at low supersaturations. They therefore may be dependent on a specific dislocation array for their growth and only occur under slow growth conditions in cirrus and in the absence of water cloud.

Dimension and axial ratios show considerable variability. Ono (1969) and Auer and Veale (1970), from formvar replicas, found that plates and dendrites have a thickness 30-60 μm, greater diameter (5 mm) crystals being thicker; the variability of thickness for a given size is $\sim$20%. Similarly, crystal diameter for columns varied from 10 to 100 μm, the thicker columns being longer, $\sim 10^{3}$ μm. Transistion temperature growth forms occurred as thick plates with axial ratios $\sim$2 to 5. These observations were in convective or orographic cloud. Measurements in cirrus by Heymsfield and Knollenberg, 1972, and Heymsfield, (1975 a, b, c) show a variety of crystal forms, with both high (4) to low (1) axial ratio, hollow columns and bullet crystals and bullet rosettes. Mixtures also occurred in the same air parcel, of columns (75%) with plates (25%).

The origin of the ice crystals in cirrus unicus is suggested by Heymsfield (1975c) to be associated with the initial dilution of soluble particles, as cloud condensation nuclei (CCN). These highly concentrated drops grow from solid soluble nuclei, as the relative humidity first reaches $\sim$70 to 80%; these droplets, supercool well below the homogeneous freezing temperature for water ($\sim -40^{o}C$) by more than $20^{o}C$, depending on the solution molality. As the relative humidity increases with the ascending air, drops dilute, the largest diluting first, and freeze by homogeneous nucleation, as the equilibrium melting point rises. At these low temperatures the crystal texture of such drops is polycrystalline so that subsequent growth from the vapor will be in the form of spatial columns (or rosettes) as is observed.

Laboratory studies have shown that drops (mm) and cloud droplets (50 μm) freezing at temperatures below $-8^{o}C$, and $-12^{o}C$ respectively show a progressive tendency for polycrystallinity from several to several hundred different orientations depending on the degree of supercooling and size. As the freezing drops

grow from the vapor, crystals of different axial directions form, growing radially outward. At lower temperatures (-30°C) radial hollow columns, with five or so columns (bullet rosettes) are common; orientations unfavorable for growth are eliminated by mutual competition. At higher temperatures (-15°C) radial dendrites are found (Parungo and Weickmann, 1973; Heymsfield, 1973; and Kikuchi and Ishimoto, 1974). The external boundary surface for such arrays is nearly spherical showing that they probably fall without preferred orientation. An analagous phenomenum occurs with drops accreted on plates or dendrites at low temperature; these freeze with changed orientation and grow with new dendrites out of the plane of the original crystal. At low riming rates these grow into the fall direction for a horizontally oriented plate crystal; at somewhat higher riming rates these grow into the wake, with the leading edge of the crystal becoming rimed. This process has been suggested as the origin of conical graupel, where accreted drops on small oriented falling plates grow as a cone (apex angle 70-90°) into the air stream. An alternative origin for such cones has been suggested by Knight and Knight (1973). A dendrite riming with narrow cones at each tip may break under the aerodynamic stress, to shed such cones with angles 30-50°, which are sometimes observed. Growth of graupel has been shown by Mossop and Hallett (1974), and Hallett and Mossop (1973) to be associated with the production of secondary ice crystals at temperatures between -3°C and -8°C providing droplets diameter <13 μm and >25μm are present in concentration of >100 cm^{-3} and 1 cm^{-3} respectively. Maximum production rates are $\sim$1 crystal for 50 large drops accreted. These crystals may subsequently grow from the vapor and begin accreting cloud drops to form new graupel particles; alternatively they may be collected by large supercooled raindrops by hydrodynamic capture, to freeze and grow as graupel to produce yet further splinters (Hallett, et al., 1978).

As graupel particles increase in size and fall velocity, at a size 1 to 2 cm dimension, tumbling begins and growth takes place with approximately spherical symmetry. Growth instability into the airstream occurs from sizes of few mm upwards caused by enhanced collection efficiency at irregularities, which grow at the expense of the neighboring regions. The size of such an instability is related to the particle fall velocity and the drop size distribution of the supercooled cloud; spicules of different dimensions result.

Falling ice particles, conical graupel, plates or columns become oriented when the wake stabilizes the fall motion. This typically occurs with reverse

eddies which are stably attached to the rear of the falling particle, typical with Reynolds' Number of 20 to 200, the exact value depending on the particle shape. Larger particles oscillate as eddies are shed, and planar shapes eventually tumble with Re $\gtrsim$500 (snow crystals) and $\gtrsim$5000 (graupel). Smaller particles are oriented by the symmetrical flow to Re $\sim$0.1, below which they fall slantwise, along their length. In air this lower limit is somewhat hypothetical as small ice particles become randomly oriented by Brownian motion for sizes up to at least 10 μm.

The exact size where these different fall regimes are to be found, characterized for a given shape by the Reynolds' Number, and depends primarily on the particle terminal fall velocity (Jayweera and Mason, 1965; Podzimek, 1965).

Oriented particles give rise to optical phenomena which can be utilized to assess some aspects of crystal shape and size, since in general larger particles have a sufficiently large fall velocity and high Reynolds' Number to become oriented. This orientation gives rise to differential scattering in polarized radar and lidar returns, so that the presence of such oriented particles can readily be detected. Some difficulty arises in the case of lidar scattering that depolarization also occurs by multiple scattering in any water cloud present (P12). The complexities of particle shape and size distribution appear to preclude further significant information being deduced from these techniques.

Particle Density

The density of a particle may be defined in terms of its mass and external dimensions and in particular whether the particle approximates to a cylinder (column), disc (plate), or sphere. The maximum density of ice is 0.92 Mg m^{-3} (g cm^{-3}) (density relative to water .92) with lower densities occurring when growth from the vapor is in the form of hollow columns or plates, or as skeletal forms, such as needles or dendrites. Densities in the latter case have been determined in the laboratory by Ryan et al. (1974, 1976) for vapor grown crystals grown at water saturation over the range of temperature -1°C to -20°C. These results show minimum densities of 0.4 where the crystal habits are most extreme near -4°C and -15°C, compared with 0.8 to 0.9 at intermediate temperatures, where the habit is near isometric. These studies were limited by the time available for growth in their laboratory chamber. An estimate of the effective

densities of hexagonal dendrites, such as the dorite with six thin branches without side arms, as shown, for example, in Bentley and Humpheries, p 152 (1962) gives densities, estimated from the dimension and ice area with uniform thickness as low as 0.02. This is probably an underestimate as the central region of these particles are sometimes slightly separated doubled dendrites/plate of which only one grows (Jiusto and Weickmann, 1973); the overall density is estimated to be $\sim$ 0.05. Similar considerations apply to spatial arrays of columns, dendrites, or plates, with essentially a spherical external periphery. Estimates of the density of cirrus crystals collected in silicone oil by Heymsfield and Knollenberg (1972) vary between 0.6 and 0.9; crystals are bullets (probably originally from spatial rosettes) with lengths $\sim$500 μm and width $\sim$100 μm. Higher densities are associated with higher temperature cloud, 0.85 between -35°C to -22°C compared with 0.7 between -50°C to -30°C, implying that at higher temperatures the columns approximate to the solid prismatic form. (Heymsfield, 1972).

As soon as vapor grown particles begin to accrete cloud droplets, the local density changes, its value depending on the packing and spreading of the frozen droplets. Spreading depends inversely on the supercooling (T_s) and is proportional to impact velocity (V) and drop diameter (d) (Brownscombe and Hallett, 1967; Macklin and Payne, 1968). Laboratory studies of Macklin (1962) showed that the density of rime increased from 0.1 to 0.9 with increase of dV/T_s according to:

$$\rho_i = 0.11 \left(\frac{dV}{2T_s}\right)^{.76} \text{ Mg m}^{-3} \qquad \begin{matrix} d, \mu m \\ V, ms^{-1} \end{matrix}$$

With $\rho_i \rightarrow$ pure ice (.92) as $(dV/2T_s)$ exceeds $\sim$80. This latter circumstance dramatises the growth of larger hail stones diameter greater than 1 cm in higher liquid water content clouds, typical of cumulonimbus convection; densities of such hail stones are usually measured to be within 5% of pure ice (List, Murray and Dyke, 1972).

Direct measurement of mass of particles of known external dimension is achieved by capture of the particle in a suspending medium such as silicone oil which is warmed to melt the particle to a single spherical drop. This process is evidently tedious, and requires a subjective classification of the original particle and its degree of riming. A survey of this work is given in Hallett (1976). It should be pointed out that the measured mass for particles of

apparently identical size and description is liable to an uncertainty of at least a factor of three and in some cases a factor of five; this uncertainty is worst for graupel particles diameter 1-2 mm. This spread evidently reflects an inability to uniquely distinguish the internal structure from the external appearance of the particle. Locatelli and Hobbs (1974) successfully used this technique for larger (mm) graupel particles. They found a significant spread of mass for apparantly similar particles of a given size. The range of densities observed vary widely from 0.05 to 0.8 and evidently represent the range of accretion condition of Macklin's 1962 work. Difficulties arise for smaller particles ($< 20\mu m$) because of ice and water dissolution in the oil, which cannot be adequately compensated with temperature variation imposed to melt the particles.

Optical and Infrared Interaction

Optical and infrared scattering properties can be utilized under specific conditions to give an estimate of the total mass of particulate present. This follows from the relation of the scattering of spherical particles uniquely to their mass with a fixed refractive index and wavelength (Chýlek, 1978). This can be accomplished by mesurement of extinction under conditions which approximate Mie scattering with

$$\alpha = \frac{\pi d}{\lambda} \lesssim 5$$

πd = particle circumference, λ = wavelength (Pinnick et al., 1974, Gertler and Steele, 1980)

For visible light this limits particle diameter to somewhat less than 1 μm whereas utilization of a CO_2 laser at λ = 10.6 μm enables this measurement to be made with particles up to $\sim$15 μm diameter.

For ice particles within these size ranges complications first arise from the extreme habit. Of somewhat less importance in this scattering regime is the internal structure of the ice, which is likely to be in the form of small bubbles or internal surfaces which, with a d^6 scattering dependence, would tend to be a small fraction of the overall scattering. These contributions lead to a possible utilization of this technique only in the case of ice fog or a lenticular cloud with near spherical particles produced by droplet freezing at low temperature ($<-40^{o}C$) and under condition where vapor growth is a minimum.

Measurement of the scattered light and its depolarization has been utilized to distinguish between ice and water clouds remotely by lidar backscatter (Harris, 1971; Derr et al., 1976; Platt, 1977; Gibson et al., 1977; Sassen, 1978; Smiley, 1980; Smiley and Morley 1980). Depolarization results from the numerous internal reflection from facets and scattering from smaller internal crystalline facet and bubbles in rimed particles; complications arise from preferred orientation of crystals falling in a specific Reynolds' number regime (Platt, 1975) and from depolarization resulting from multiple scattering when optically thick water cloud is also present (Pal and Carswell, 1973; Derr, 1980). Detection of specular reflection from individual external crystal facets, (as opposed to the integrated scattering from many crystals in a volume with change of polarization) give the possibilities of remote assessment of crystal habit, size and concentration, (Sassen, 1977). The technique relies on some knowledge of the orientation frequency of the crystals (and hence their fall Reynolds Number), with a difference in depolarization of light scattered from columns and plate crystals, and direct measurement of the individual optical pulses from specular reflections. Complications arise from non-uniformities of size and shape of crystals in a given sample volume, and probably from different internal structures in plates or in columns under different growth conditions.

There does not appear to be much hope for determination of crystal mass by this technique, which would require use of an empirical assessment of particle density with problems already discused. Perhaps the greatest problem is that the lidar visibility is limited as soon as water cloud is present, and gives only information at the cloud periphery, which for cumulus is $\lesssim$100 m and extensive water cloud gives depolarization through multiple scattering. An identical problem exists for utilization of any inversion technique for utilization of radar backscatter for crystal distribution.

Mechanical Aspects of Particle Impaction

Large ice particles (several mm) falling at terminal velocity at the ground can be seen to bounce or fragment on impact, although smaller crystals (½ mm) often survive intact as they settle slowly on to even a hard surface. Vardiman (1978) has shown that pristine crystals survive intact after falling at terminal velocity on a hard surface, whereas, moderately rimed particles gave as many as ten secondary particles on such a collision. At aircraft velocities, particles $\sim$mm dimension are observed to collapse on impact near a stagnation point, where, in the absence of further collection, they evaporate.

Little work has been carried out on the detail of this impaction and evaporation process. At aircraft velocities, snow stick observations show that particles ½ to 3 mm are accreted in a "collapsed" condition; larger ice particles, are deflected, but whether break-up occurs is unknown. Studies of fractured particles on the formvar replicator show that break-up occurs for plates greater than a few hundred microns diameter at impaction velocities $\sim$100 ms^{-1}; graupel particles and three dimensional crystal arrays of size up to 2 mm often break on impact to give a crater like deposit; in each case the material appears to be retained near the impaction site (Hallett, 1976).

Simple theory of bounce shows that under conditions of elastic impact only, ice particles impacting with ice rebound in about 1 μs; (Hertz rebound); laboratory studies have shown that actual contact time for bouncing particles is significantly greater. This implies that processes other than elastic impact occur - interaction with adsorbed layers may be important for small crystals and crystal fracture and plastic flow for large particles. The process is complicated (see Bowden and Tabor, 1950; Ackley, 1973) and it appears that prediction of the process of ice particle impaction and break-up on theoretical grounds is highly unsatisfactory, if only for the reasons, first that the initial particle properties - diameter, mass, size, and internal structure of the ice are subject to a wide variability, and second that the impact gives rise to unknown local rise of temperature of the ice at the impaction site. It is concluded that impaction characteristics per se do not offer much opportunity for particle characterization.

This survey of ice in the atmosphere points out the inherent problems which arise in attempting characterization of ice particles from aircraft or surface sensors. This results from the lack of uniqueness in any correlation between the gross properties -- size, shape, mass and the resulting inherent lack of utility in use of single physical measurements of ice using a single sensor. This difficulty is compounded by the large spread in particle size and mass, which predicates a wide dynamic range in sensing instrumentation. These problems are examined in specific cases in the following section.

PART II: INSTRUMENTATION

AIRCRAFT COLLECTION TECHNIQUES Direct Capture (1)*

Collection of ice particles in flight and their subsequent analysis is the obvious technique to utilize in an ice particle investigation. Techniques have utilized a forward facing aperature exposed to the air stream which leads to a low angle ($<5^{o}$) diverging channel such that particles sediment, and are collected in a refrigerated vessel. The vessel may contain hexane (flammable) or a low viscosity silicone oil to reduce evaporation and sintering. Problems arise by shattering of particles on impact on the intake edge and on other internal surfaces. Even though the airflow of such systems can, in principle, be made isokinetic by adding a converging section at the rear, attitude changes of the aircraft lead to uncertainties in the rate airflow by $\sim$2. Sequential samples can be taken during flight with a practical time resolution $\sim$10 seconds. The onerous task of subsequent data analysis in the laboratory renders this technique only suitable for occasional spot sample checks; and, it follows that unrepresentivity of the sample becomes a serious problem under most atmospheric sampling conditions. Thus, spatial resolution is limited; a collection period may vary from a fraction of a second to several minutes. This technique works best for individual ice particles, but presents problems for colliding of snow flakes (or graupel) in the tunnel shear; local motion of the collection fluid can cause snow flake break-up.

Particles can be examined in microscopic detail to give dimensions, structure and crystal axes using polarized light. After examination, each particle can be transfered to a separate vessel and melted (slowly) to give a spherical water droplet where size gives the mass of the initial particle. For small particles (10 μm) it is necessary to utilize a suspending oil in which water solubility is low, otherwise dissolution can become a problem, when the specimen is not measured or photographed immediately after collection. Prior saturation of the oil with water partly overcomes this problem; but temperature changes, to melt particles can still lead to significant dissolution as in general the water solubility increases with increase of temperature.

A variation of this technique, most appropriate for smaller particles ($<$100 μm) is to use a refrigerated microscope slide covered with a layer of higher viscosity (10-100 cs) silicone oil. This is exposed directly to the air

* numbers refer to Appendix A

stream for a short period and stored for subsequent analysis. Particle shatter is a problem for larger sizes; smaller sizes (10 μm) may not be collected or fail to penetrate the oil. The latter situation can be improved by exposing the slides in a decelaration section of a wind tunnel outside or inside the aircraft.

Collection, Snow Stick (2a)

An alternative to such a "soft landing" capture technique is to collect particles on a surface at higher velocities, (possibly with some deceleration from aircraft speed), with the detailed analysis carried out on the particle at its collection site. A modification of this technique records the ice as a plastic replica or a crater in aluminum foil for subsequent analysis. The simplest of these devices is the "snow stick" a black rod one cm in diameter which protrudes beyond the aircraft boundary layer and is readily visible by the observer. A black surface, with a scale, provides a background for collection. Visual assessment gives the presence, and approximate size and concentration of ice particles. Rotating the stick from inside the aircraft enables a fresh surface to be exposed as one surface becomes covered. This technique gives yes/no criteria for the presence of ice particles. With an area 2 cm^2, air speed 100 ms^{-1} this sweeps 20 ℓs^{-1}. The visual resolution is ∿0.5 s, giving an upper concentration limit of 1 to 10 particles ℓ^{-1}. Particles may shatter on impact, with a shattered opaque particle visual lower limit ∿¼ mm. This implies that graupel and three dimensional crystal arrays will be counted most effectively; single, transparent crystals least effectively.

This technique works only in the absence of rime formation which seriously reduces the contrast of impacted particles. The tedium of observer recording is the most serious problem of this technique. Improvement of this could be achieved by continuous T.V. recording/filming of the stick as the barrel of a microscope with internal optics; this latter technique has been used effectively in laboratory studies for monitoring particle fallout. It is necessary to heat the surface somewhat above ambient temperature so that a particle evaporates prior to arrival of the next one; it would be necessary to servo a collector heater, probably via an optical sensor. This technique, in the first instance, requires manual data analysis and evaluation, with its attendent time problems, although automatic data handling is definitely possible. This would, at a minimum, require

a survey of ice centers and size at a set time interval (say one second) such that a new set of particles are accreted; this gives a mean of the particle concentration and size (through calibration) over $\sim$100 m of flight path.

Impaction on Heated Surface (2b)

A modification of this technique has some possibility for mass size correlation and mass number distribution. The evaporation rate of accreted particles depends on the local undersaturation with respect to the environment. With accretion at the stagnation point, this is enchanced by dynamic heating (some $4^{o}C$ at 100 ms^{-1}) to give an undersaturation of = $\sim$20% at $-15^{o}C$. This could be further enhanced by additional heating which would make the evaporation rate less dependent on environmental saturation, which, in cloud, would lie between water and ice saturation. Evaporation times of such particles are estimated (Appendix B). Utilizing only stagnation temperature increase, this gives for solid ice particles:

Particle Diameter	Time for Evaporation
mm	5s
100 μm	½s
10 μm	.05s

This gives a lower limit of $\sim 10^{-7}$ g with a lower limit of time resolution of .001s.

Commercially available TV systems typically operate at picture scan frequencies of $\sim$1/30 s, which would give a lower size limit $\sim$10 μm for a particle visibile on one scan only. In practice it would be desirable to locate it on two scans, giving a practicable limit of $\sim$20 μm equivalent diameter. A faster scan system to record the statistics of the lengths of time (number of scans) for which each particle persists, and giving a distribution over appropriate time intervals would then give a mass distribution. Problems arise in estimating mass from evaporation time, but it should be possible to achieve a laboratory calibration, using ice spheres of known size. Most commercial TV scan systems have a persistance which lasts over several scans; a short persistant tube may be required. It appears that the software necessary for this data processing and display is currently available commercially (e.g., Quantimet Systems). An

alternative viewing technique would consist of using a coherent fiber optic bundle to convery the optical image into the aircraft. Illumination can be carried in the same bundle. American Optical Co., Southridge, MA make several versions. In particular, a fiber as small as 8 μm can be made with 83% core, and 17% cladding. A 1 cm diameter bundle, 2-3 feet long would cost ∿ $3K.

Foil Sampler 2(c)

This technique operates continuously with a thin metal (aluminum) foil strip being exposed to the airstream, through a deiced slot, for a suitable period. The foil is moved over a gauze mesh such that the impact gives a shape with direct size calibration. This is convenient for raindrops; it can be utilized to record impacts of graupel and crystalline particles, recognizable for size down to about ½ mm. Instruments with apertures up to 10 cm^2 are practical with a sample rate ∿100 ℓs^{-1}. Visual analysis is required; this is tedious and time consuming.

It can be speeded up by use of various semi-automated systems by use of a TV system with light pen to identify and count suitable particles. Ice crystal forms need to be assessed qualitatively by the analyst which introduces some subjectivity into the results.

Replica (2d, e)

Weickmann first utilized replica technique for recording cirrus crystals, utilizing a microscope slide covered with varnish exposed from an open cockpit of a low speed aircraft. The varnish was allowed to dry at low temperature (Weickmann, 1947). This technique gave good quality replicas. Continuous replication, using a 16 mm film leader coated with formvar chloroform solution was subsequently utilized (MacCready and Todd, 1964). At higher aircraft speeds (>80 m s^{-1}) increasing problems of crystal fracture and shatter occur (summary, Hallett, 1976). Some improvement can be achieved by a deceleration system, although there is a greater uncertainty in the concentration (Hobbs et al., 1974) The data require visual analysis and interpretation. Sampling rates are ∿1 ℓs^{-1}, through a slot 2 mm wide. Spatial resolution of ∿20 cm can be achieved with film transport rates of 60 cm s^{-1}.

General Comments - Class 2 Techniques

Each of the techniques described above requires a high degree of skill, both in the data collection and in its subsequent analysis. The continuous

collection systems (foil, Formvar) are in principle capable of utilizing automated analysis techniques by TV scan and appropriate software; indeed such systems are available commercially and are employed in metallurgical and aerosol analytical techniques. Shapes can be recognized and the software programmed for obtaining appropriate statistics of concentration, size, and shape. These techniques have not been developed for ice crystal analysis, which reflects in part the very wide natural variability of crystal shapes, sizes and concentrations, which are likely to occur. The problem is compounded by the uncertainties introduced by the impact shatter crystals and of artifact grown after replication. Visual assessment of this is quite possible, but presents a formidable problem in automating the analysis. Automation of the measurement of the size of accreted particles near a stagnation point and their subsequent evaporation appears as a distinct possibility. The lower particle limit is $\sim 10^{-7}$ g (<100 μm dimension), the upper particle limit will be set by particles which bounce on impact, rather than collapse as an ice heap, which is 10^{-3} g, $\sim$2 mm diameter.

OPTICAL TECHNIQUES

Direct Photography (3)

Perhaps the most direct method for examination of ice particles in the atmosphere is by in situ photography of the falling particle. A choice exists, as with all optical systems, between resolution and field of view, to be specified by the consideration of particle concentration and size (fig. 1). For sharp images, airspeed correction is necessary. This was achieved by the device of Cannon, 1975. The resulting image is necessarily limited by depth of focus. This problem can be reduced by a recently developed technique utilizing two different color beams (red and green) intersecting in the image plane. Color photography shows in focus yellow particles, whereas out of focus particles appear as red or green and can be readily rejected in analysis (Cannon, 1980). Estimate of particle concentrations can be obtained from knowledge of the field of view and depth of focus of the optical system gives a sample volume 0.1 to 1.0 ℓ. A mean size may be inferred from the image characteristics, a mass determination made from utilization of a density inferred from the particle type. This requires tedious analysis, together with a degree of subjectivity, both in the assessment of the particle classification and in its density.

In principle, automatic analysis techniques may be applied to the photographs to give concentration and size; these developments have not been carried out to any significant extent since the two dimensional imaging techniques described later gave this information in a way which can be recorded on tape and subsequently processed.

Holography (4)

In principle, holography could provide better answers than photography as its three dimensional capability permits thickness measurements for some crystal orientations. Additionally, the depth of field is much larger than that obtainable with a photographic method, since the whole sample volume can be reconstructed. A practical instrument (Conway et al., 1980) has sample volume $\sim \frac{1}{2}\ell$, and an effective resolution ~ 15 μm in reconstruction, with samples obtained at 1 s intervals. A specific advantage of this instrument is that it records particles in an approximately spherical volume, as opposed to the long thin sample volume examined by direct sampling instruments and other imaging instruments, and the thin slice of direct photography. This is advantageous for investigation of the local spread of particle characteristics as opposed to the spatial averaging produced by other techniques.

Data handling and reduction are difficult and, in addition, being an imaging technique, hollow crystals are not always distinguishable. Estimation of crystal mass requires the same level of skill and has the uncertainties as that of direct photography.

Electro Optical Imaging (5)

A commercially available instrument developed by Knollenberg (Knollenberg, 1976; Heymsfield, 1976) determines the size and shape of particles with a two-dimensional shadowing technique. A helium-neon laser beam width 2.1 mm, shadows particles on an optical array with spatial resolution ~ 25 μm.

A choice exists between resolution and field of view. Two models are commerically available models OAP-2D-C,OAP-2D-P, Particle Measuring Systems, Boulder, Colorado which give a maximum image height ~ 750 μm or ~ 6 mm. Sampling rate is $\sim$ liters s^{-1}; the slice elements are scanned at a 4 MHz rate. This system gives a great advantage of automated data recording and analysis.

Hard copy print-out of particle projected images can be readily obtained; software can be written to give shape, size and projected area distributions. In principle, masses can be estimated from the cross-sectional area and knowledge of crystal types and inferred density. The crystal thickness is not known and there is a problem with hollow crystals, as in the previous two methods. Software classification of crystals to assign a mean density and mass from the projected shape is subject to the uncertainties of classification and variability described earlier. Minimum particle size detected requires coverage of two array elements; in practice, to identify a crystal, this requires rather more elements in the direction at 90^{o} to the minor axis; a practical resolution rather better than $\sim$100 μm is achievable. Particles with circular cross-section may be supercooled drops, frozen drops, low density graupel or, disc crystals. Ice particles which are single crystalline or composed of a few large crystals may be distinguished from liquid by estimating the phase retardation by the ice of light of different direction of polarization; velocities of light propagation differ along "a" and "c" crystal axis. This technique works in principle and practice for particles which do not have internal or bubble structure (as graupel). Some difficulty may therefore arise in differentiation between spherical graupel and spherical water drops < mm dimension. Larger drops are deformed in fall with flat bases, which give a ready identification of phase. Difficulties arise in using polarization techniques for small particles in high cloud droplet concentration, which may give a depolarized signal resulting from multiple scattering (R. Hobbs, private communcation). Real time output of ice particle parameters is possible (Stickle and Booker, 1980).

Development of these electro optical probes has given a new opportunity for assessment of ice particle size and concentration, in cirrus and convective clouds. Heymsfield (1975) used early versions of this instrument; more recent studies have been reported by Varley 1978a, b, Varley and Brooks, 1978; Varley and Barnes, 1979; and Cohen, 1979. Results give ice water content estimated from "typical" particle densities, approaching 0.1 g m^{-3}; particles often appear as rosettes, sometimes larger than 1 mm in dimension and concentrations of all sizes of a few particles per cm^{-3}. Extensive studies of graupel and larger vapor grown particles in convective clouds have been carried out, for example, Cerni and Cooper (1980). The utility of these instruments is greatest for ice particles minimum dimension $\gtrsim$ 100 μm; smaller ice particles occurring in ice fogs and

in the initial stages of secondary ice production in convective clouds may escape detection. It should be noted that the foreward scattering spectrometer probe (F.S.S.P.) manufactured by Particle Measuring Systems is also sensitive to ice particles, but yields counts in all channel sizes, presumably related to the multitude of individual protubances of different sizes on individual ice particles.

Differential Doppler Measurements (6)

This technique consists of overlapping two CW coherent beams originating from the same laser. A spatial fringe pattern is formed which becomes the sample volume. Radiation scattered by particles going through the fringe pattern is measured. The particles modulate the scattered radiation with a frequency determined by the particle velocity and the fringe spacing. Particles larger than the fringe spacing produce incomplete modulation according to their size relative to the fringe separation. Hence, particle velocity and size above a threshold value can be determined. However, mass is not determinable from these measurements unless particles are spherical and the density is known.

Optical Scattering (7)

These techniques use the principle of measuring light scattering in the forward (or other) direction of polarized light. In general, water drops do not depolarize the light on scattering. An instrument has been described by Turner and Radke (1973) which counts the crystal concentration. It discriminates between drops and crystals, although problems arise in depolarization of light from deformed raindrops and coalescing cloud drops. It is not useful for mass, or size determination as the signal intensity is related, in an unknown way, to the particle density and crystal orientation; this orientation is in general arbitrary during observation.

Optical Imaging Technique for Ice Crystal Mass Determination (8)

The technique described in 2(b) for mass estimation utilizing the evaporation time for an ice particle accreted near an aerodynamic stagnation point can be improved in resolution, both in time and location on the accreting surface by optical techniques more complex than the vidicon system described above.

The three methods available are:

(a) Direct impact on a heated linear or square array.

(b) Direct impact on a heated array with alternate sensors and illuminators.

(c) Direct impact on a heated surface imaged by either an optical system and an electrically-scanned matrix sensor array or a mechanically and electrically scanned sensor array-mirror combination.

Method (a) with a matrix sensor array would be a simple method, however, the smallest center-to-center spacing of sensor elements in available photodiode arrays is about 40 μm (a fundamental limit) in both X and Y directions which is too large for measurement of small crystals. Linear arrays are available with 15 μm center-to-center spacing with 1872 sensors (EG & G, Reticon, model RL1873F). The array by itself would have an effective collection area of only $4 \times 10^{-3} cm^2$ which is not large enough to be useful. Method (b) listed above is not useful for this application for the same reasons. The third method appears to be the only one worth considering. This method requires an electronically-scanned matrix array or an electronically scanned linear array in conjunction with a mechanically scanned mirror with a separate impact surface.

A Matrix Array Camera

A matrix array could essentially be used in a camera with a lens chosen for the proper magnification and off-the-shelf electronic micro-circuits used for control circuitry and data aquisition. The arrangement is shown in fig. 2. Arrays with 100 x 100 (10,000 photodiodes) and 60 μm center-to-center spacing and a 256 x 256 (65,536 elements and 40 μm spacing) are available from EG&G, Reticon (model RA 256 x 256). The sensor sizes are 0.6 x 0.6 cm and 1 x 1 cm respectively so a system with 1:1 magnification using the 256 x 256 array would provide a collection area of 1 cm and resolution in the object plane of about 40 μm or sampling rate of $10\ \ell s^{-1}$ and at 3:1 magnification the resolution and sampling rates are 13 μm and $1\ \ell s^{-1}$ at an aircraft speed of $100\ ms^{-1}$. The resolution can be increased simply by increasing the magnification of the optical system but the sampling area goes down accordingly. A magnification of 2:1 has a resolution of 20 μm and a sampling area of only 0.25 cm^2 or sampling rate of $2.5\ \ell s^{-1}$ and at 3:1 magnification the sampling area is only 0.11 cm^2. Several arrays could be used to give enchanced sampling areas.

The maximum number of looks at the collection plate per second is determined by the maximum rate at which the array can be scanned which is

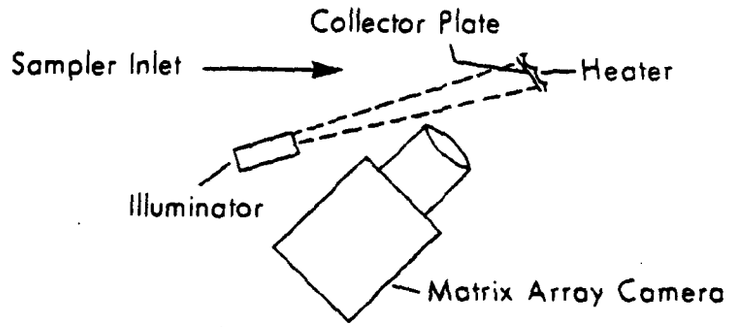

OPTICAL IMAGING TECHNIQUE WITH MATRIX ARRAY CAMERA

Fig 2 Conceptual diagram of an airborne optical scanning ice crystal mass measuring instrument employing a matrix array camera and heated impact - evaporation plate.

at a pixel rate of 10 MHz. At this rate one frame can be scanned in 6.55 ms. corresponding to a frame rate of 153 frames s^{-1}, this is to be compared with the standard vidicon of 30 frames s^{-1}.

A Linear Array Camera

The sampling rate-resolution trade-off situation can be improved by using a linear array which has more closely-spaced elements in a camera with a mechanically scanned mirror to move the image in a direction perpendicular to the linear array. Electro-magnetic mirror scanners are available (Bulova, type L50) with 1 cm apertures and 5^{o} peak-to-peak angular excursion rates of up to 400 Hz. The mechanical and electronic scan rates could be synchronized so that with 1:1 magnification, a sample area of 1 cm^2 could be covered once every 2.5 ms with a resolution of 15 x 15 μm and sampling rate of 10 ℓs^{-1}. A scheme using a linear array camera is shown in Fig. 3.

Comparison of Matrix and Linear Array Camera Schemes

For equivalent resolution of 15 μm the linear array system offers a high sampling rate - 10 ℓs^{-1} compared to 1.4 ℓs^{-1} for the matrix camera and a larger maximum frame rate -- 400 frames s^{-1} compared to 153 frames s^{-1}. However, the scheme employing the linear array is more complex mechanically and problems could occur from vibrations affecting the scanning mirror, while the matrix method can be made very rugged since no moving parts are required.

Data acquisition for the two schemes is discussed below. The matrix array is on a chip which also contains the scanning electronics. Each photodiode is interrogated sequentially within a line. Each line is subsequentially accessed.

A controller is available which controls the array scan, processes the analog video and presents analog and binary-coded digital outputs with 6 or 8 bit resolution. A CRT can be attached directly for real time viewing and the digital output can be interfaced with a microcomputer for digital processing and data recording.

Data handling for the linear array is slightly more complicated as the mechanical scan and electronic scan must be synchronized. Electronically the operation is very similar to the matrix scheme.

The question of the length of time actually required between looks at the collector plate is important from the standpoint of frame rate required.

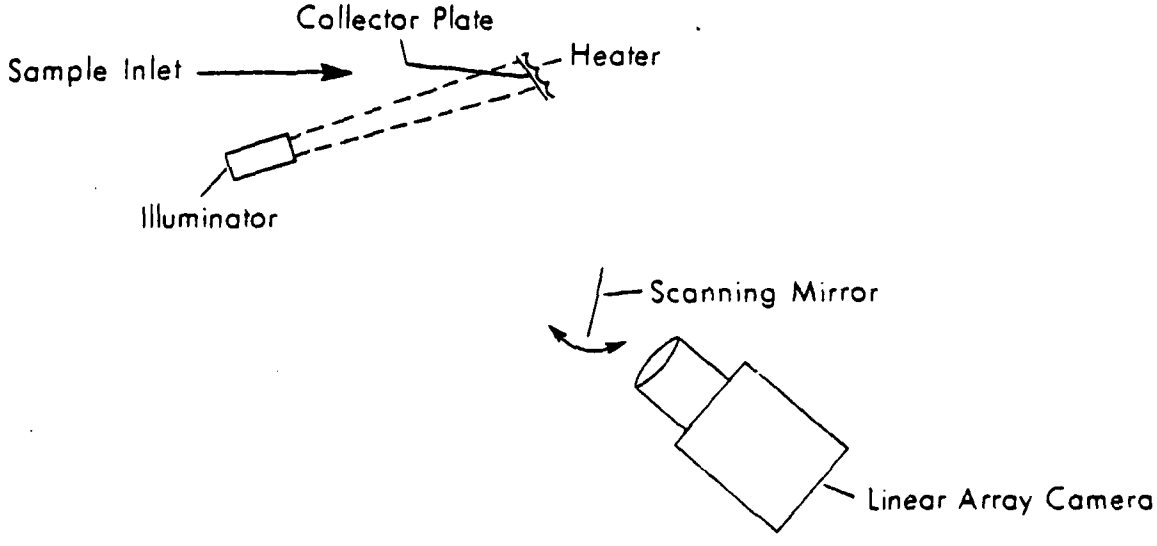

OPTICAL IMAGING TECHNIQUE WITH LINEAR ARRAY CAMERA

Fig 3 Conceptual diagram of an airborne optical scanning mass measuring instrument employing a linear array camera with scanning mirror and heated impact - evaporation plate.

The important time element is the length of time required to evaporate the smallest crystals. Using equations in Appendix B, t (s) = 2 x 10^4 m (g), we see that a 100 μm diameter crystal with mass of 7.2 x 10^{-9} g is evaporated in $\sim 10^{-3}$ s. This is faster than the frame rate of either the matrix or linear array schemes. A 1 mm long, 100 μm diameter crystal having 7.2 x 10^{-6} g would evaporate in about 0.1s. which is no problem in terms of frame rates. The smallest detectable crystal mass values are 5.2 x 10^{-8} g and 1.8 x 10^{-8} g respectively for the matrix array scheme and the linear array and scanning mirror scheme. If the temperature of the collector plate were decreased, the smaller crystals could be resolved with the linear array camera and scanning mirror. This could be achieved by thermo-electric cooling of the accretion site; it would only be practical for small crystal collection rates and concentrations. Direct collection of crystals on the array would eventually be destructive, so a surface protective plate would be required. To prevent loss of resolution this must be thin and may require occasional replacement.

Optical Systems

For the matrix camera, a convenient set of numbers for the image distance, D_i, object distance, D_o, and focal length, f, for the lens are: D_i = 50 D_o = 25 cm and f = 16.67 cm. This gives a magnification, M, of M = 2. for the linear array camera with scanning mirror, a magnification of M = 1 can be used and convenient optical parameters would be D_i = 25, D_o = 25 cm and f = 12.5 cm.

Alternatively a coherent fiber optic bundle might be used instead of the lens system to convey the image to the detection array. See the discussion under snowstick collection, page 17.

Crystal Evaporaton and Vapor Pulse Detection by Lyman-alpha Observation (9)

This technique requires that the ice crystal be evaporated and absorbtion measured in the pulses of water vapor produced. A wavelength must be chosen at which the water vapor absorption coefficient is very large and where there are no important coincidental absorption lines from other atmospheric gases. This rules out even the intense 2.7-μm water band as the absorption is not strong enough. At 10°C and under saturation conditions a path length of 0.22 cm will attenuate a monochromatic beam of Lyman-alpha (0.12156 μm) radiation

to e^{-1} of its original intensity (Tillman, 1965), while under the same conditions a few meters of path would be required to attenuate a beam of 2.7 μm radiation by the same amount. At 0°C the path length for e^{-1} transmission at the Lyman-alpha wavelength is 0.43 cm. An additional advantage of the Lyman-alpha wavelength is that coincidences with absorption lines of O_2 and O_3 do not interfere (see Buck, 1976).

As we will show in the following discussion, existing Lyman-alpha hygrometers are not suitable; considerable modification would be involved in order to achieve crystal-mass determination. The detector would require a higher frequency response, and modified data acquisition electronics.

Suitability of Existing Lyman-alpha Hygrometer to Measure Ice Crystal Mass.

Lyman-alpha Hygrometers have been discussed in the literature, see for example Buck (1976), Tillman (1965), and Ruskin (1976). Instruments for aircraft use have been built by Electromagnetic Research Corporation (ERC) and also by General Eastern Corporation (GEC). The GEC instrument is based on an instrument developed at the Naval Research Laboratory (Randal et al. 1965). This device has the capability of measuring total water content - vapor, liquid and ice in clouds. The entire sample is converted to the vapor state by a 400 W heater element in the probe. The water vapor is then determined by measuring the transmittance of the sample with UV - Lyman-alpha radiation over a path of 0.5 cm.

This instrument could be used to measure ice mass concentration in ice clouds, but it is not designed to determine the mass of individual crystals. This is partly because the response time is 3 ms which correspond to a 3-meter long sample for an aircraft speed of 100 m s^{-1} and an effective sampled volume of 75 cm^3. In order to measure individual crystal masses, the temporal response must be reduced to a time interval short compared to the time required for a pulse of water vapor from a single evaporated crystal to pass through the UV beam.

The expected performance of a Lyman-alpha single crystal mass spectrometer, is similar to the above but modified to include a faster detection scheme, is now determined for the following parameters: water vapor with length 10 cm (based on 0.1 s. evaporation time) and diameter, 0.5 cm from evaporator, transit time of water vapor through sampling beam - 1 ms, UV

sample beam size - 0.5 cm diameter and 0.5 cm long and a crystal 100 μm long, 10 μm in diameter (mass 0.7×10^{-8}g).

The change in water vapor density produced by the pulse from a single crystal increases the ambient value by

$$\Delta\rho = \frac{7.2 \times 10^{-9} \text{ g}}{1.96 \text{ cm}^3} = 3.67 \times 10^{-9} \text{ g cm}^{-3}.$$

The sensitivity of the instrument can be determined from Beer's Law:

$$\frac{I}{I_o} = \exp = \frac{k\rho_x}{\rho_o}$$

where R is the transmittance of a uniform sample of length x ; I and I_o are transmitted and input intensities respectively, ρ is the water vapor density (or concentration) in the sample; ρ_o is the water vapor pressure at STP; and k is the sample vapor absorption coefficient referred to STP.

According to Tillman, (1965) the value for k is 387 cm^{-1} for the Lyman-alpha radiation. An estimate of the senstivity for the above mentioned condition is calculated for STP. The change in transmission resulting from a single crystal is

$$\Delta R = \frac{-k\Delta\rho R x}{\rho_o}$$

Assuming we are starting from a condition of dry air initially, $\Delta\rho = 3.67 \times 10^{-9}$ g cm^{-3} and $\rho_o = 8.04 \times 10^{-4}$ g cm^{-3},

$$\Delta R = \frac{(387)\ (3.67 \times 10^{-9})}{(8.04 \times 10^{-4}}$$

$$\simeq 10^{-3}$$

or one part in 1000. For crystals on the other end of the scale, say 1000 μm long by 50 μm in diameter, ΔR turns out to be ~ 0.3. The latter number is easily resolvable while the former is too small to detect in this kind of experiment. Therefore, small crystals would be missed. If we assume that ΔR should be no smaller than 5%, then the smallest crystal mass detectable with this scheme is 4×10^{-7} g corresponding to a crystal having length 370 μm and 37 μm diameter.

Development of a Modified Lyman-alpha Instrument for Crystal Mass Measurement.

The Lyman-alpha liquid water content meter modified to include a faster detector and metal plate evaporator as described in the previous section was unable to measure crystal mass smaller than 4×10^{-7} g. The sensitivity can be increased by fast evaporation so that the plume is smaller in extent. This requires "flash" evaporation in a time of the order of 10^{-4} s. for the smallest crystal if the air flow is the same as the aircraft speed. If a decelerator is used, the time could be longer. For simplicity it is assumed that the evaporator is upstream from the sample measuring volume as shown in the simplistic diagram of Fig. 4 to illustrate the general concept.

If the plume going through the sample volume from a crystal of mass 7×10^{-9} g has expanded after flash evaporation and diffusion to a volume of ½ x ½ x 1 cm, then ΔR in dry ambient air would become 0.01 or more realistically in saturated air at -10°C, the ambient transmittance would be 0.56 or $\Delta R = 0.05$. In order to produce a ΔR of 5%, the crystal mass would have to be 0.7×10^{-7} g, corresponding to a crystal 220 μm long by 14 μm in diameter.

The time response of the system must be $<10^{-4}$ s. The nitric oxide ion chamber used in previously-developed Lyman-alpha hygrometers is not suitable here as its response time is several milliseconds. A photomultiplier tube with a MgF window must be used as the detector.

The signals obtained from larger crystals will depend on the detailed operation of the flash evaporation scheme, but the initial rate of evaporation could increase with crystal size by the ratio of surface areas if a CO_2 laser or other radiant field method were used. This is desireable so that the peak signal would be larger. The total crystal mass would be obtained by integrating the pulses produced and dividing by the ambient transmittance.

A possible device is depicted in Figure 4. The ice crystals enter the inlet and are identified as crystals by scattering of polarized light. The trigger produces a pulse for each crystal entering and fires a CO_2 laser serving as a flash evaporator.

It is shown in Appendix C that such a system requires a high energy density and the capability of a pulse rate at sufficiently high frequency to respond to individual crystals as they pass through the sample volume. Both

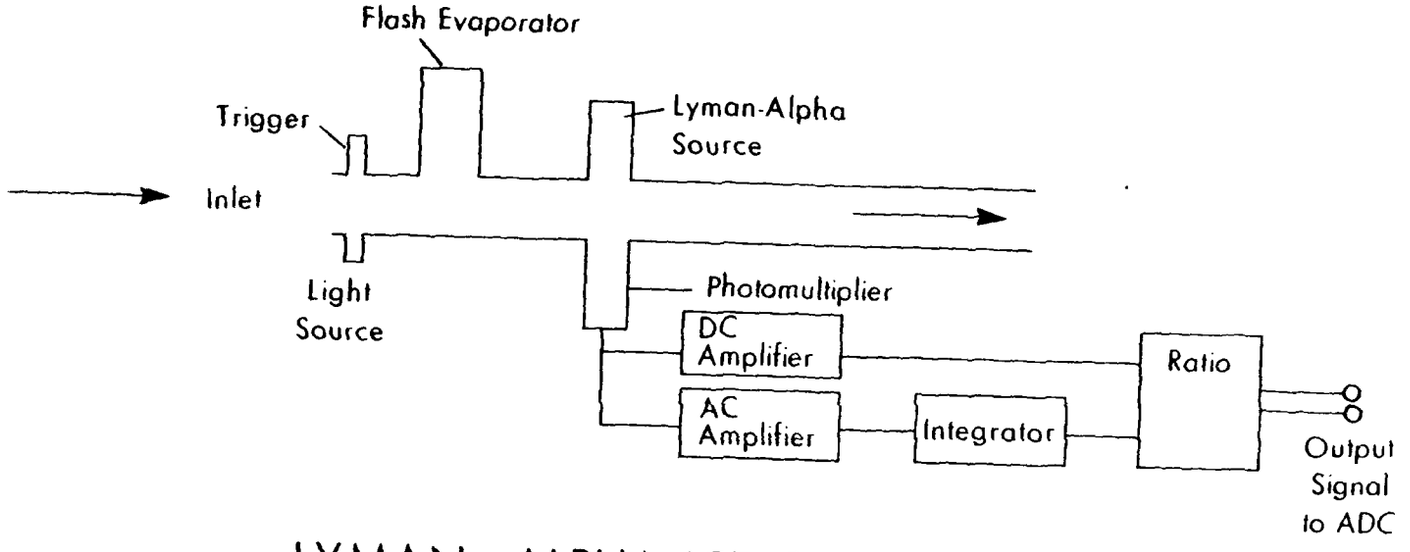

LYMAN—ALPHA ICE CRYSTAL MASS MEASUREMENT SCHEME

Fig 4 Arrangement for Lyman-alpha ice crystal mass measurement.

of these requirements present some difficulty with current technology. Other schemes for flash evaporation such as heated impact plate do not require the trigger. The Lyman-alpha source is a H_2 discharge lamp containing UH_3 which produces a pure Lyman-alpha spectrum (see Buck, 1976). The sampling rate of the scheme illustrated would be 5 ℓs^{-1}.

The H_2 lamp should work well in this application, even though it has significant beam spread, because the sample path is short. Recently coherent well-collimated Lyman-alpha laser or laser-derived sources have been developed (Cotter, 1979; Smiley, 1981) which would be required for a sample path length of several cm or longer. These longer path lengths are useful only in air with low moisture content at lower temperatures.

It is essential to know the water vapor fluctuation frequency distributions to be expected in cirrus environments in order to determine the background limited performance under various conditions. While some measurements at lower frequencies (< 1 kHz) have been made, the size of the fluctuations in the 10 kHz region are important here. At an airspeed of 100 ms^{-1} this frequency of 10 kHz is equivalent to a spatial scale of 1 cm. At cirrus levels the molecular diffusity of water vapor in air is $D \sim 0.7\ cm^2\ s^{-1}$. The relaxation time constant for a vapor element of d cm dimension is:

$$\sim \frac{d^2}{\pi^2 D} \text{ i.e. } \sim 13 \text{ seconds.}$$

Hence, over meteorological time scale such variations are unlikely in clear air. However, with large individual cirrus crystals falling in unsaturated air, moist wakes of some 10 times the crystal size could occur, and give rise to some uncertainty as they were ingested. Some crude knowledge of the maximum crystal size and mass (as could be obtained from a 2D image device) should be sufficient to assess the seriousness of this problem in a given situation.

It is assessed that while there are some unsolved problems in this technique it merits further investigation for crystal mass measurement.

THERMAL TECHNIQUES

Detection by Resistance Change on Accretion (10)

The standard Johnson Williams hot wire liquid water content meter works by accretion and evaporation of cloud drops on a hot wire which is included in

a feedback loop to maintain constant resistance (temperature), the required power being directly proportional to the net rate of drop accretion. The system gives problems for very small drops (μm) which fail to be collected at all by the wire (530 μm diameter) and larger droplets which splash to lose a significant part of their mass (diameter $\gtrsim$ 40 μm). Flight of this instrument in an ice cloud gives essentially a zero reading; it is occasionally observed to be greater than noise (0.05 g m^{-3}).

In principle it is not suitable as an ice water content meter, if only for the reason that most particles significantly exceed the wire dimension, fracture on impact and are carried away. Droplets splash when

$$L = \frac{\text{kinetic energy}}{\text{surface energy}} = \gtrsim 20;$$

thus at aircraft speed some splashing occurs for drops greater than a few μm diameter; loss of mass does not appear to be important until $L \gtrsim 200$, under aircraft conditions. Wind tunnel studies show that droplets on impaction and collection on a cold wire run around the wire periphery and are retained at the anti-stagnation point; on a heated wire local wetting and evaporation take place, with still some water running to the rear for evaporation at higher collection rates. By contrast, ice crystal impaction on a narrow wire does not appear to cause wetting (there is too little time for the ice to melt) and the particle is carried away. This is in contrast to the collection of ice particles near the stagnation point of a larger aerofoil or other obstacle, where impaction is followed by collection. This raises the question of detection of the ice accretion rate by the local cooling at the accretion site as the particle evaporates, operating on the same principle as the Johnson Williams instrument but measuring the resistance changes caused by individual accretion events. This technique would have the advantage of giving (in principle) direct mass measurement. The basic limitation will be interference by simultaneous or near simultaneous collection. The time constants for evaporation will be of the same order as those computed in Appendix B; the cooling will spread into a typical sensing surface with a time constant $\sim$0.01 s.

Collection of a 100 μm ice particle (mass 10^{-6} g) on a strip target 10 mm, width 1 mm, with a sample rate at 100 ms^{-1} of 1 ℓs^{-1}, gives a fractional

resistance change, assuming that ½ of the evaporation heat comes from the collector, of 10^{-3} for a thermally isolated nichrome collector. Higher sensitivity can be achieved using a semiconductive material, but more problems arise with material erosion for direct impact. Commercially available thin metal film detectors on ceramic substrates are also available (e.g., Omega Engineering, Pt 100 Fkt 3/10).

It is estimated that this unit would have a time constant 0.1 s, but would probably be liable to degradation under continuous ice crystal impaction. With the geometries discussed above, a limitation exists of a few particles per liter; mass detection would be determined by the sensitivity of low resistive measurement, but $1:10^3$ at a 10^{-6} g of ice appears to be a lower limit. Problems of particle edge collection by this technique could be removed by a guard ring to reject signals when activated.

This technique has the advantage, as does (2b) that the quantity measured is directly related to the vaporization latent heat and the particle mass.

Replicator Melting (11)

Two possibilities were examined for determination of ice mass by prior melting of the ice and subsequent measurement of the size distribution of the resulting droplets. The most simple of these is to melt ice collected in the fomvar choloroform solutions of a continuous replicator, allow it to dry in the usual way, and determine the drop size distribution by detailed counting (tedious) or by an automated system. This has problems already discussed relative to particle break-up on impaction; ice fragments of the original crystal would not melt back together. Edge shatter would also present serious problems, which could not be removed by use of decelerator systems.

Cavity Melting (12)

An alternate technique would be to melt particles in a thermal radiation cavity and then measure the drop size distribution, using, for example, the forward scattering spectrometer probe (F.S.S.P.) manufactured by Particle Measuring Systems, Boulder, Colorado. This technique presents problems when a size distribution of ice particles is present, as sufficient heat to melt larger particles will entirely evaporate smaller ones.

Alternatively, individual crystals may be melted separately by triggering a CO_2 laser as discussed in Appendix C. Even here, estimating the required pulse to melt and not evaporate a crystal provides a problem since the mass of the crystal is obviously required and this is the unknown in the first place. In view of these difficulties and the large spread of some ice spectra this concept was not pursued further.

MECHANICAL TECHNIQUES

Momentum (Ballistic) Balance (13)

In this scheme a crystal impacts with a very light movable mirror which is one reflector for a Fabry-Perot interferometer. The collision causes the interferometer mirror and the impacted crystal to move with an initial velocity which is measureable by counting fringes per unit time. The mass of the crystal can then be determined from the conservation of momentum if its impact velocity is known. It appears that this technique is not suitable for aircraft measurements as turbulence in the airstream and aircraft vibration are too large: the delicacy of such an impact optical device appears quite unsuitable for aircraft speed operation. The latter problem can be readily demonstrated by consideration of the mass of an eddy in a turbulent boundary layer at 1 cm from the stagnation point. With a cm "sausage" eddy this gives a momentum change mv, where v is $\sim$ aircraft speed and the eddy volume is $\sim 10^{-4}$ cm^3 or mass 10^{-7}g. Thus crystals above 10^{-6} g could be detected by this technique; the general delicacy of the sensor is however a severe problem.

Microphone Pickup (14)

Similar considerations apply to this technique as the ballistic balance, although the microphone is subject to much more rugged construction and could be mounted near a stagnation point. Practical considerations of isolation from aircraft acoustic noise suggest that this technique would be very difficult to realize.

Detuning of a Mechanical Resonator by Crystal Collection (15)

Aircraft icing detection systems employ a resonating probe consisting of a cylinder exposed at right angles to the airstream which collects and freezes supercooled water drops; these, in turn, reduce its frequency. Periodically the

probe is heated and deiced; the heating frequency is taken as a measure of the icing rate (Rosemount Engineering, Inc.). High sensitivity in such a system is achievable with a measurement of frequency of $\Delta f/f$ of $1{:}10^6$. A cylinder exposed normally to the airstream collects along its length so that identical mass gives a detuning depending on the site of impaction; vortex eddy shedding gives a frequency which approximates the natural period of a probe of practical dimensions. This geometry is therefore highly undesirable. For small changes it is necessary to add the mass to the tip of the vibrating system, so that ideally the probe would need to be exposed at the stagnation point of the aerofoil with its surroundings deiced. For such an oscillating system, it can be shown that:

$$\frac{\Delta f}{f} = -\tfrac{1}{2} \frac{\delta W}{(W + .2\ wL)}$$

f - frequency, w = mass/unit length of sensor, L = length (first harmonic) δW is an additional mass on a tip load W. At 10 kHz this gives $\delta f \sim 0.1$ Hz, or an accuracy of $1{:}10^5$.

This is high and can be achieved with long (10^3 Hz) measuring time; it is somewhat doubtful if it would work with crystal evaporating over 1 s or less. Some further investigation of this technique does, however, seem appropriate.

ELECTRICAL TECHNIQUES

Contact Charging Devices (16)

Problems with aircraft telecommunications are often caused by corona discharge when the aircraft has become highly charged on collision with snow particles. This effect has been studied experimentally by Stimmel et al. (1946), Shaefer (1947) and Dunham (1965). The question arises as to whether contact electrification can be used to advantage in ice crystal investigations as it has in the investigation of concentrations and sizes of aerosols (Guyton, 1946).

Ice particle detectors based on contact electrification have been produced by Mach and Hobbs (1969) and McTaggart-Cowan et al. (1970). Both these devices have been used to measure ice particle concentrations by observing the electrical pulses generated when ice particle collided with a short length wire. In order to develop the system so as to obtain information about the properties of the ice crystals it would be necessary to investigate experimentally the magnitude and sign of the pulse generated when ice crystals of various habits

and sizes collide with the wire at aircraft velocities. Problems would be encountered in the field due to existing charges on ice crystals which on passing close to the detector would induce charge in the wire, or, on collision transfer some of its existing charge. It may be possible with a recording system of sufficient resolution to discriminate between the different types of events (Tanner and Nanevicz, 1956) but the problem remains as whether an ice crystal of a given habit and mass would produce a unique signature on collision with the detector.

The physical mechanism of charge transfer when ice makes contact with a metal is not known. McTaggart-Cowan et al. report that the type of wire used in their detector had little effect on the amount of charge separated. However, Buser and Aufdermaur (1974) found strong correlation between charge transfer and metal work function when 20 - 40 μm diameter ice spheres were allowed to collide with different metal targets. If charging is proportional to work function then difficulties would arise in producing a detector with a known and constant work function as this quantity can be drastically altered by oxide layers and other surface conditions. Buser and Aufdermaur also found that charging was dependent upon the impurity concentration of the ice. They did not investigate the effects of temperature and humidity on the charge transfer process but the surface properties of ice are known to be highly temperature dependent. Anderson and Hallett (1979) have shown that humidity also has an effect on the ice surface and influences the charge magnitude and sign following crystal impacts of ice on ice (Hallett and Saunders 1979). It is also probable that the charge separated on collision is proportional to the contact area which would vary depending upon orientation of the crystal at the moment of contact.

The theory of devices that have been used to size water droplets by measuring the change in capacitance of an electrode due to the presence of the droplet have been discussed by Winn (1968). Again, it does not appear that a similar device could be usefully designed for use with the ice phase since the change in capacitance would be a function of the linear dimensions and orientation of the crystals rather than of a unique quantity such as mass.

In conclusion, because so little is known at this time about the physical mechanism of the charge transfer process on ice/metal collisions, it seems unlikely that a contact charging device could be designed to give unambiguous information about ice crystal mass or habit.

Microwave Refractometer (17)

This method requires that the ice crystals first be completely evaporated and then the water vapor plume analyzed with a microwave cavity refractometer. It appears that the dilution factor (the volume of a reasonable-sized cavity divided by the volume of water vapor produced by a single crystal) is much too large to permit the scheme to work except for crystals larger than 200-300 μm (10^{-5} g). Larger particles take much longer to evaporate than smaller ones, and the natural spread of particle size therefore gives a spread of vapor plumes which interact with an effective time resolution of ∿0.1 s of air in the resonant cavity. Moisture fluctuations of this order from the atmospheric variability of both temperature and water vapor will give rise to problems and confusion of interpretation (Cunningham, 1963). This technique does not give promise.

REMOTE TECHNIQUES

Optical Scattering Methods

Indirect determination of the characterization by optical scattering methods might involve scattering or backscatter (lidar) with consideration of polarization effects and optical phenomena.

Lidar (18)

Optical radar or lidar techniques (Collis, 1970) measure backscatter. This has been shown to be a useful technique for determining the presence and structure of ice clouds and also for discriminating qualitatively between ice and water particles (using depolarizaton measurements) in clouds (Sassen, 1978; Platt, 1977; Smiley et al., 1977). However, it does not appear likely that mass can be determined. Doppler lidar can measure the fall velocity of crystals from which mass could be determined if the particles were spherical. Crystal habit influences fall velocity (see, for example, Heymsfield, 1972) therefore crystal types must be known for any assessment of total mass. In general, lidar beam volumes are much too great to investigate individual crystals, although Sassen (1977) has utilized individual specular reflections to give information on crystal concentration when orientation effects can be determined independently.

Optical Phenomena (19)

Optical phenomena such as sun dogs, $22\frac{1}{2}^{o}$ and 46^{o} haloes, sun pillars, and targential arcs are refractive effects while coronae are caused by diffraction (see, for example, Minnaert, 1954). These phenomena are not appropriate for determining crystal mass; the refraction effects depend on crystalline angles and crystal orientation and can therefore give some indication of crystal size throuigh the Reynolds' number of the falling particles (Glass and Varley, 1978). Diffraction can, in principle, provide some information on crystal size but is useful only when the sizes and types are nearly the same, and the shapes are nearly spherical which is usually not the case.

It is generally concluded that optical phenomena and lidar techniques do not give quality of information required for mass determination.

PART III: CONCLUSION

It is concluded that techniques are currently available for concentration measurement of ice particles. Various imaging systems, which have automated data handling capability, enable size and shape of particles to be similarly obtained, with some uncertainty of their third dimension (probably not a serious problem) but considerable uncertainty about the internal structure. Both scattering and imaging techniques are fundamentally unsound for mass; scattering techniques are fundamentally unsound for shape and size. Particle evaporation with UV detection of the vapor plume possibly merits further study. A more promising potential exists for impaction and time history of evaporation for both size (using optical scan) and mass using the time history of evaporation of accreted particles either examined optically, or by cooling and change of electrical resistance, or accretion and detuning a resonant oscillator. Each technique has the capability of automated data handling. The principle suffers from uncertainties of particle disintegration on impact and its sensitivity to the air speed and orientation of the flow at the sensor site; its advantage lies in measurement of a quantity unambiguously related to particle mass.

APPENDIX A

TECHNIQUES FOR CHARACTERIZATION OF ATMOSPHERIC ICE PARTICLES

DIRECT TECHNIQUES - AIRBORNE

AIRCRAFT COLLECTION TECHNIQUES:

	Principle	Direct Information	Indirect Information	Advantages	Problems	References
1. Direct capture	decelerate and store	all		detailed analysis of original particle possible	tedious analysis; representitivity; particle fracture	Schreck et al., 1974
2. Collection	(a) snow stick	size (½ mm) concentration		quick visual evaluation	limited data	various
	(b) particle accretion on heated surface; recorded at 1/30 s intervals.	concentration mass	size	automated mass distribution output	calibration of mass; particle bounce, and irregular contact with accreting surface.	new concept
	(c) metal foil	size, concentration habit	mass (inferred density)		particle fracture; time consuming analysis .	Garrod, 1957; Cannon et al., 1974 Knight et al., 1977 .
	(d) Formvar replica	shape, concentration	mass (inferred density)	permanent record	particle fracture; time consuming analysis.	Weickmann, 1947
	(e) continuous formvar replication	shape, concentration	mass (inferred density)	continuous permanent record	complex instrument; particle fracture; time consuming analysis	MacCready & Todd, 1964; Hobbs et al, 1974 Hallett, 1976
OPTICAL TECHNIQUES						
3. Direct Photography	airborne camera, airspeed compensated	projected habit and size; concentration	mass (inferred density)	surface detail resolved	tedious analysis depth of focus limitation	Cannon, 1975; Cannon, et al., 1974
4. Holography		Habit, size, concentration	mass (inferred density)	sample volume - entirely in focus and near spherical	analysis technique complex and tedious	Kunkel, 1971
5. Electro optical	shadow on optical array	projected size and shape	mass (inferred density)	automated analysis of shape and size	small size cut-off	Heymsfield, 1976; Knollenberg, 1976
6. Differential Doppler Scattering	spatial interference pattern; differential Doppler Shift	size, velocity		size and velocity determined independently	only valid for spherical particles; small size cut-off	
7. Optical scattering	Scatter, polarized light	concentration			spurious scatter and depolarization of large drops	Turner and Radke, 1973

	Principle	Direct Information	Indirect Information	Advantages	Problems	References
8. Optical imaging collection on hot surface	time for image of crystal on hot plate to disappear	size; energy required to evaporate crystal		direct measure of mass	calibration of mass	new concept
9. Lyman-alpha absorption	evaporate crystals measure, absorption at 1215 A	mass		direct readout of mass size distribution	source, windows, temporal response; background water vapor variability vaporization technique	Buck, 1976; Ruskin, 1976
THERMAL TECHNIQUES						
10. Collection on hot surface	resistance change	mass		direct measure of mass	calibration; damage to surface	new concept
11. Melt collected ice particles on replicator	drop size, distribution measured	mass			original particle fracture on impaction; edge collection	
12. Thermal radiation cavity to melt ice	drop size distribution measured optically	mass		direct mass measurement	preferential evaporation of small particles; power requirements	new concept
MECHANICAL TECHNIQUES						
13. Impart momentum loss	ballistic balance (interferometric)	momentum	mass	direct mass measurement	aerodynamic turbulence	new concept
14. Acoustical pickup	direct, impact microphone	momentum	mass	direct mass measurement	difficult signal processing to give mass aerodynamic turbulence	Joss and Waldvogel, 1967
15. Detune a resonant system	impact on heated resonating surface	mass		direct mass measurement	particle break-up; sensitivity	
ELECTRICAL TECHNIQUES						
16. Charge loss on impaction	charged wire sensor	mass	shape		self-induced charge on impaction; unknown capacitance effects; variable contact potential	Mach and Hobbs, 1969; McTaggert-Cowan, Lala and Vonnegut, 1970; Winn, 1968
17. Microwave techniques	evaporate crystals determine water vapor in refractometer	mass	resolution of individual particles		dilution factor too large	Cunningham, 1963
REMOTE TECHNIQUES						
18. Backscatter, lidar	direct and depolarized specular reflections	volume scattering x-section; discrimination between ice and water	relative amounts of ice and water		anomalous response to certain orientations; no mass sensitive parameter	Collis, 1970; Platt, 1975; Sassen, 1978; Smiley, 1977
19. Optical phenomena	refraction and diffraction of solar radiation by crystals	crystal angles; limited orientation information; limited size information			Only useful for sizes when near monodisperse condition exists	Glass and Varley, 1978; Tricker, 1979

APPENDIX B

Evaporation Rate of an Ice Particle Accreted Near the Stagnation Point

The evaporation of an ice particle accreted on a snowstick or leading edge of the wing is readily viewed from inside the aircraft and can be recorded. The evaporation time can, in principle, be used as a measure of the crystal mass. This relationship can be computed subject to some simplification.

1. At aircraft speed ($\sim$100 ms^{-1}) the ice particle is flattened to a disc radius r, density ρ_c, and thickness T.
2. The crystal is accreted near the stagnation point and at aircraft speed the boundary layer thickness (δ) is small compared with the accreted crystal dimension.

$$\delta \sim \frac{x}{Re^{1/2}} \qquad \text{where } x = \text{crystal dimension}$$

   Re 625, with typical values, and $\delta \sim x/25$ hence, to a first approximation, the crystal is ventilated at the ambient airspeed.
3. The crystal thermal capacity is small compared with that of the accreting metal surface.
4. The crystal temperature is the same as that of the accreting surface. This is a reasonable assumption with sparse accretion on a high thermal conductivity metal surface.
5. The mass evaporation rate of the particle is given by

$$\frac{dm}{dt} = 4\ \pi C\ D\ F\ (\rho_s - \rho_\infty)$$

C = electrostatic capacity = $\frac{2r}{\pi}$ (for a disc)

D = Vapor diffusivity of water vapor in air
(0.2 $cm^2\ s^{-1}$ at 1000 mb)

F = Ventilation coefficient
$1 + 0.27\ Re^{1/2}$

ρ_s = Vapor density of ice at the surface temperature

ρ_∞ = Vapor density of ice in the environment, which, under conditions of ice accretion will be the saturated vapor density of the environment.

$\sigma = \frac{\rho_s}{\rho_\infty}$ = is under saturation with respect to the environment, providing the driving force for evaporation.

In terms of the disc radius, or mass this becomes, for the time to evaporate from a radius r or mass m, to r_o, m_o.

$$t = \frac{\pi T \rho c}{4 D F \rho_\infty (\sigma - 1)} (r - r_o)$$

or

$$t = \frac{1}{8 D F \rho_\infty (\sigma - 1)} (m - m_o)$$

The temperature of the accreting surface may be near the stagnation temperature (by dry adiabatic compression in a sparse cloud of large ice crystals) $\sim 4^\circ C$ excess at 100 m s^{-1} velocity or it may be deliberately heated and servoed above this value.

Taking typical conditions, $-10^\circ C$, flight velocity 100 m s^{-1}, particle Reynolds number, 625.

$D = 0.2$ cm^2 s^{-1}, $T = 50$ μm, $\rho_c = 0.1$ g cm^{-3}

$\rho_\infty = 2 \times 10^{-6}$ g m^{-3} dynamic heating $\sim 4^\circ C$,

and neglecting change of ventilation as the particle becomes small,

$t \sim 50$ r seconds, (r, cm)

$t \sim 2 \times 10^4 m$ seconds (m, g)

For a mm particle, this is a time $\sim$ 5s

100μm $\sim$ ½s

for a $\frac{1}{2} .10^{-4}$ g particle, a time $\sim$ 1 s

With 0.001 s time resolution and spatial resolution of 10 μm, this gives a lower limit of detection of $\sim 10^{-7}$g.

It is pointed out that mass calibration would be independent of assumption of crystal density. The basic measurement will be the time for each particle to evaporate "completely," i.e., to the limit of the optical detection system or the temperature detection system, as appropriate. These times can be shortened by heating the collector; this is probably necessary to remove problems of icing up in high ice collection rates or in supercooled water situations.

APPENDIX C

Laser Requirements for Melting and Evaporating Ice Crystals in Aircraft Instrumentation

Assume carbon dioxide laser operating at 10.6 μm and absorption coefficient = 1 for both ice and water.

Melting

(a) Rate of change of energy

$$\frac{dE}{dt} = \frac{c_i\, m_c\, \Delta T + L_i\, m_c}{t}$$

where c_i = specific heat of ice

m_c = mass of crystal = $\frac{4}{3}\pi r_c^3 \rho_i$

ΔT = temperature change up to $0^\circ C$

L_i = heat of fusion for ice

t = time required to melt crystal

(b) Laser beam intensity required

$$\frac{dE}{dt} = I\, A_c$$

where I = laser beam intensity

A = cross sectional area of crystal

Assuming a spherical ice crystal radius r at a temperature of $-10^\circ C$

$$I\,\pi r^2 = \frac{4}{3}\pi r_c^3 \ell_i \left(\frac{c_i\, \Delta T + L_i}{t}\right)$$

where $c_i = 0.55$ cal g^{-1}

$L_i \sim 80$ cal g^{-1}

$\rho_i \sim 0.92$ g cm^{-3}

which gives

$$I = \frac{440r}{t} \text{ W cm}^{-2}$$

Time required for ice crystal to travel at velocity V through beam dimension D, with D = 1 cm and V = 100 m s^{-1}

$t = 10^{-4}$ sec.

Then

$$I = 4.4 \times 10^6 \, r_c \ W \ cm^{-2}$$

when L is vaporization latent heat at 100°C. For a 500 - μm radius crystal,

$$I = 2.2 \times 10^5 \ W \ cm^{-2}$$

A cw laser cannot provide this amount of power so a pulsed laser must be used.

(c) Energy requirements for a pulsed laser

The energy flux required to melt a 500 μm crystal in a 1 cm diameter beam is It or

$$It = 2.2 \times 10 \ j \ cm^{-2}.$$

This is still too stringent a requirement for a practical system so the beam diameter must be reduced. This also reduces the transit time, so the energy requirement goes down only as the beam diameter. A 1 mm beam would require 2.2 J in a 2×10^{-5} s (or shorter) pulse.

Another alternative is to use a rectangular beam shape with a 1 cm length and 2 mm diameter, when

$$E \cong 4 \ j \text{ in } 2 \times 10^{-4} \ s$$

Evaporation

Additional energy beyond melting for a drop

Rate of change of energy

$$I \, A = \frac{dE}{dt} = \left(\frac{c \ m \ \Delta T}{t}\right)_{0\text{-}100^\circ C} + \left(L \frac{dm}{dt}\right)_{T = 100^\circ C}$$

where L is the vaporization latent heat at 100°C.

For 0.2 x 1 cm beam and 500 μm radius drop and $t = 10^{-4}$s this gives:

to raise temperature 4 J.

to vaporize 91J.

Hence, for 500 μm radius crystal, assumed spherical, in beam 0.2 x 1 cm,

$(E)_{tot.} = E_1$ (raise crystal temperatures from $-10^{o}C$ to $0^{o}C$)
$+ E_2$ (melt crystal)
$+ E_3$ (raise drop to $100^{o}C$)
$+ E_4$ (evaporate drop)

$(E)_{tot.} = 99J$ (in $2 \times 10^{-4}s$)

For a 100 μm ice crystal, this is $(E)_{tot.} = 20$ J

Laser Source Required

The energy requirements are high, ∿100J pulse to evaporate 500 μm radius crystals. It would be necessary to trigger the laser by incoming crystals. The maximum pulse rate would have to be fairly low, perhaps 1 - 5 Hz for a practical size in the laser power supply. CO_2 lasers with higher repitation rates, as high as 2.5 kHz, and pulse length $10^{-4}s$ are available, but would be excessivly large for aircraft use.

REFERENCES

Ackley, S.F. 1973: Microhardness testing on ice single crystals. Physics of Chemistry of Ice, Whalley, Jones and Gold (Eds.), Roy. Soc. Canada, 382-386.

Anderson, B.J., and J. Hallett 1979: Influence of environmental saturation and electric field on growth and evaporation of ice crystals. J. Cryst. Gr., 46, 427-444.

Auer, A.H., and D.L. Veal, 1970: The dimension of ice crystals in natural clouds. J. Atmos. Sci., 27, 919-926.

Barnes, A.A., 1978: New Cloud Physics Instrumentation Requirements, Fourth Symposium, Meteorological Observations and Instrumentation, American Meteorological Society, Denver, 264-268.

Bentley, W.A. and W.J. Humphries, 1962: Snow Crystals. Dover Publications, p. 151.

Bowden, R.P. and D. Tabor, 1950: Friction and lubrication of solids. Ch. XIII, Nature of Contact Between Colliding Solids, p. 258-284.

Brownscombe, J.L. and J. Hallett, 1967: Experimental and field studies of precipitation particles formed by the freezing of supercooled water. Roy. Met. Soc. Quart. J., 93, 455-473.

Buck, A.L. 1976: The variable path Lyman-alpha hygrometer and its operating characteristics. Amer. Met. Soc. Bull., 57, 1113-1118.

Buser, O., and A.M. Aufdermaur, 1974: Electrification by Collision of Ice Particles on Ice or Metal Targets. Proc. Int. Conf. on Atmospheric Electricity, Garmisch-Partenkirchen.

Cannon, T.W., 1975: A photographic technique for measurement of atmospheric particles in situ from aircraft. J. Appl. Met., 14, 1383-1388.

Cannon, T.W., J.E. Dye and V. Toutenhoofd, 1974: The mechanism of precipitation formation in northeastern Colorado cumulus. II Sailplane Measurements. J. Atmos. Sci., 31, 2148-2151.

Cannon, T.W., 1980: A color camera for in situ photography of cloud particles. J. Appl. Met., 19, 898-900.

Cerni, T.A. and W.A. Cooper, 1980: Ice Crystal Concentrations in Isolated Cumulus Clouds of Montana. Proc. VIII Cloud Physics Conference, Clermont-Ferrand, France, 195-198.

Chylek, P., 1978: Extinction and liquid content of fogs. J. Atmos. Sci., 35, 296-300.

Cohen, I.D., 1979: Cirrus Particle Distribution Study, Part 5. AFGL-TR-79-0155.

Collis, R.T.H., 1970: Lidar. Appl. Opt., 9, 1782-1788.

Conway, B.J., A.H. Bentley, and M. Kitchen, 1980: Results from the Meteorological Office; Airborne Holographic Particle Measuring. Proc. 8th Int. Cloud Physics Conf., Clermont-Ferrand, p. 661-664.

Cotter, D., 1979: Coherent UV source for the Lyman-alpha region. Opt. Commun., 31, 397-400.

Cunningham, R.H., 1963: The microwave refractometer used and humidity sensor in cloud physics. Humidity and Moisture, Vol. 12, Ch. 74., p. 615- 627, Wexler (Ed.), Reinhold Pub. Corp., New York.

Derr, V.E., N.L. Abshinen, R.C. Cupp, and G.T. McNice, 1976: Depolarization of lidar returns from virga and source cloud. J. Appl. Met., 15, 1200-1203.

Derr, V.E., 1980: Estimation of the extinction coefficient from multi-wavelength lidar backscatter measurements. Appl. Opt., 19, 2310-2314.

Dunham, S.G., 1965: Electrostatic charging by solid precipitation. J. Atmos. Sci., 23, 412-415.

Garrod, M.P., 1957: Recent developments in the measurements of precipitation particles from aircraft. Met. Res. Papers, London, 1050.

Gertler, A.W. and R.L. Steele, 1980: Experimental verification of the linear relationship between the extinction and liquid water content of clouds. To be published.

Gibson, A.J., L. Thomas and S.K. Bhattachorgya, 1977: Some characteristics of cirrus clouds deduced from laser-radar observations at different elevation angles. J. Atmos. and Terr. Physics, 34, 657-660.

Glass, M., and D. Varley, 1978: Observations of Cirrus Particle Characteristics Occurring with Halo. Conf. on Cloud Physics, Issaquah, WA, A.M.S., 126-128.

Guyton, A.C., 1946: Electronic counting and size determination of particles in aerosols. J. Ind. Hyg. Toxicol, 28, 133-141.

Hallett, J., and B.J. Mason, 1958: The influence of temperature and supersaturation on the habit of ice crystals grown from the vapor. Proc. Roy. Soc., A, 247, 440-453.

Hallett, J., 1963: Experimental studies of the crystallization of supercooled water. J. Atmos. Sci., 21, No. 6, p. 671-682.

Hallett, J., and S.C. Mossop, 1973: Production of secondary ice particles during the riming process. Nature, 249, 26-28.

Hallett, J., and C.P.R. Saunders, 1979: Charge separation associated with secondary ice crystal production. J. Atmos. Sci., 35, 2230-2235.

Hallett, J., 1976: Measurement of size, concentration and structure of atmospheric particulates by the airborne continuous particle replicator. AFGL-TR-76-0149.

Hallett, J., R.I. Sax, D. Lamb, and A.S.R. Murty, 1978: Aircraft measurements of ice in Florida cumuli. Roy. Met. Soc. Quart. J., 104, 631-651.

Harris, F.S., 1971: Water and ice cloud discrimination by laser beam scattering. Appl. Opt., 10, 732-737.

Heymsfield, A.J., 1972: Ice crystal terminal velocities. J. Atmos. Sci., 29, 1348-1357.

Heymsfield, A.J., 1973: Laboratory and field observations of the growth of columnar and plate crystals from frozen drops. J. Atmos. Sci., 30, 1650-1656.

Heymsfield, A.J., 1976: Particle size distribution measurement: An evaluation of the Knollenberg optical array probes. Atmos. Tech., 8, 17-24.

Heymsfield, A.J., and R.G. Knollenberg, 1972: Particles of cirrus generating cells. J. Atmos. Sci., 29, 1358-1366.

Heymsfield, A.J., 1975d: Cirrus unicus generating cells and the evolution of cirriform clouds, Part I, Aircraft observations of the growth in the ice phase. J. Atmos. Sci., 32, 799-808.

Heymsfield, A.J., 1975b: Cirrus unicus generating cells and the evolution of cirrus clouds, Part II, The structure and circulation of the cirrus unicus generating head. J. Atmos. Sci., 32, 809-819

Heymsfield, A.J., 1975c: Cirrus unicus generating cells and the evolution of uniform clouds, Part III, Numerical computations of the growth of the ice phase. J. Atmos. Sci., 32, 820-830.

Hobbs, P.V., R.J. Farber, and C.J. Joppa, 1974: Collections of ice particles from aircraft using decelerators. J. Appl. Met., 13, 522-528.

Jayaweera, K.O.L.F., and B.J. Mason, 1965: The behavior of freely falling cylinders and cones in a viscous fluid. J. Fl. Mech., 22, 709-720.

Joss, J.V. and W. Waldvogel, 1967: Ein spektrogrpah fur Niedersclagstropfen mit automatischer Auswertung. Pure and Appl. Geophys., 68, 240-246.

Jiusto, J.E. and H.K. Weickmann, 1973: Types of snowfall. Amer. Met.Soc. Bull., 54, 1148-1162.

Keller, V.W., and J. Hallett, 1981: Influence of air velocity on the habit of ice crystals grown from the vapor. To be published.

Keller, V.W. and R.I. Sax, 1981: Microphysical development of a pulsating cumulus tower. Roy. Met. Soc. Quart. J. In Press.

Keller, V.W., C.F. McKnight, and J. Hallett, 1980: Growth of ice discs from the vapor and the mechanism of habit change of ice crystals. J. Cryst. Gr., 49, 458-464.

Kikuchi, K., 1970: Peculiar shapes of solid precipitation observed at Syowa Station, Antarctica. J. Met. Soc. Japan, 68, 243-249.

Kikuchi, K., 1971: Peculiar shape of snow crystals of Antarctic type observed at Hokkaido. Geophys. Bull., Hokkaido Univ., 25, 167-180.

Kikuchi, K. and K. Ishimoto, 1974: Role of frozen cloud droplets on the growth of snow crystals of certain shapes. J. Fac. Sci., Hokkaido Univ, Series VIII (Geophysics), 4, 69-80.

Knight, C.A. and N.C. Knight, 1973: Conical graupel. J. Atmos. Sci., 30, 118-124.

Knight, C.A., N.C. Knight, W.W. Grotewold and T.W. Cannon, 1977: Interpretation of foil impactor impressions of water and ice particles. J. Appl Met., 16, 997-1002.

Knollenberg, R.G., 1976: Three New Instruments for Cloud Physics Measurements; The 2-D Spectrometer, the Forward Scattering Spectrometer Probe, and the Active Scattering Aerosol Spectrometer. Proc. Int. Cloud Physics Conf., July 26-30, Boulder, CO, 554-561.

Kobayashi, T., 1965: Vapor growth of ice crystals between -40°C and -90°C. Met. Soc. Japan J., Ser. II, 43, 359-367.

Kobayashi, T., 1957: Experimental parameters on the snow crystal habit and growth by means of a diffusion cloud chamber. Met. Soc. Japan J., 75th Anniv. Vol.

Kunkel, B.A., 1971: Fog drop-size distributions measured with a laser hologram camers. J. Appl. Met., 10, 482-486.

List, R., W.A. Murray, and C. Dyke, 1972: Air bubbles in hailstones. J. Atmos. Sci., 29, 916-920.

Locatelli, T.D., and P.V. Hobbs, 1974: Full speed and masses of solid precipitation particles. J. Geophys. Res., 79, 2185-2197.

Mach, W.H., and P.V. Hobbs, 1969: The Electrical Particle Counter, Contributions from the Cloud Physics Group; Research Report III, Results of Aircraft Measurements in Winter Storms (1968-1969); Over the Cascade Mountains, Univ. of Wash., 80-95.

Macklin, W.C., 1962: The density and structure of rime formed by accretion. Roy. Met. Soc. Quart. J., 88, 30-50.

Macklin, W.C. and G.S. Payne, 1968: Some aspects of the accretion process. Roy. Met. Soc. Quart. J., 94, 167-175.

MacCready, P.B., and C.J. Todd, 1964: A continuous particle sampler. J.Appl. Met., 3, 450-460.

McKnight, C.V. and J. Hallett, 1978: X-ray topographic studies of dislocations in vapor grown ice crystals. J. Glacio., 21, 397-407.

McTaggart-Cowan, J.D., G.G. Lala, and B. Vonnegut, 1970: The design construction and use of an ice crystal counter for ice cloud studies by aircraft. J. Appl Met., 9, 294-299.

Minnaert, M., 1954: The Nature of Light and Color in the Open Air. Dover Publications, Inc., New York.

Mossop, S.C. and J. Hallett, 1974: Ice crystal concentration in cumulus clouds: Influence of the drop spectrum. Science, 186, 632-634.

Ono, A., 1969: The shape and riming properties of ice crystals in natural cloud. J. Atmos. Sci., 26, 138-147.

Pal, S.R. and S.R. Carswell, 1973: Polarization properties of lidar backscattering from clouds. Appl. Opt., 12, 1530-1535.

Parungo, F.P. and H.K. Weickmann, 1973: Growth of ice crystals from frozen cloud drops. Beiträge zur Physik der Atmosphäre, 46, 289-304.

Pinnick, R.G., S.G. Jennings, P. Chylek, and H.J. Auvermann, 1974: Verification of a linear relation between I.R. extinction, absorbtion and liquid water content of fogs. J. Atmos. Sci., 36, 1577-1586.

Platt, C.M.R., 1975: IR emission of cirrus simultaneously with satellite lidar and radiometric observations. Roy Met. Soc. Quart. J.,101, 119-126.

Platt, C.M.R., 1977: Lidar observations of a mixed-phase altostratus cloud. J. Appl. Meteor., 16, 339-345.

Platt, C.M.R., 1975: Lidar backscatter from horizontal ice plate crystal studies. J. Atmos. Sci., 17, 482-488.

Podzimek, J., 1965: Measurement of Ice Particles in the Atmosphere. Proc. Cloud Physics Conf., Met. Soc. of Japan, Tokyo, 226-230.

Randal, D.L., T.E. Hanley and O.K. Larison, 1965: The NRL Lyman-alpha humidiometer. Vol. I, Principles and Methods of Measuring Humidity in Gases. Wexler A. and R.E. Ruskin (Eds.). Reinhold Pub. Corp., New York, p. 428-443.

Ruskin, R.E., 1976: Liquid water content devices. Atmos. Tech., 8, 38-42.

Ryan, B.F., E.R. Wishart, and E.W. Holroyd, 1974: The densities and growth rates of ice crystals between -3°C and -9°C. J. Atmos. Sci., 31, 2136-2141.

Ryan, B.F. and E.R. Wishart, and D.E. Shaw, 1976: The growth rates and densities of ice crystals between -3°C and 21°C. J. Atmos. Sci., 33, 842-850.

Sassen, K., 1977: Ice crystal habit discrimination with the optical backscatter depolarization technique. J. Atmos. Sci., 16, 425-431.

Sassen, K., 1978: Air truth lidar polarization studies of orographic clouds. J. Appl. Meteor., 17, 73-91.

Schaefer, M.J., 1947: Properties of particles of snow and the electrical effects they produce in storms. Amer. Geophys. Union Trans., 28, 587-614.

Schreck, R.I., V. Toutenhoofd, and C.A. Knight, 1974: A simple, airborne, ice particle collector. J. Appl. Meteor., 13, 949-950.

Smiley, V.N., 1980: Antarctic Journal of the U.S. To be published.

Smiley, V.N., 1981: High power tunable lasers for the UV, visible and IR. Advances in Electronics and Electronic Physics, Academic Press. To be published.

Smiley, V.N., B.M. Morley, and J.A. Warburton, 1977: Lidar and replication studies of ice crystal precipitation at the South Pole. Antarctic Journal of the U.S., XII, 166-167.

Smiley, V.N. and B.M. Morley, 1980: Lidar depolarization studies of the atmosphere at the South Pole. To be published.

Stickel, P.G. and Booker, R.D., 1980: Real Time Processing of Cloud Particle Image Data. Proc. 8th Int. Conf. on Cloud Physics, Clermont-Ferrand, 725-728.

Stimmel, R.G., E.H. Rogers, E.F. Waterfall, and R. Gunn, 1946: Electrification of aircraft flying in precipitation areas. Proc. IRE, 34, 167-177.

Tanner, R.L., and J.E. Nanevicz, 1956: Radio noise generated on aircraft surfaces. Final Report Contract AF 33(616)-2716 SRI Project 1267.

Tillman, J.E., 1965: Water vapor density measurements utilizing the absorption of vacuum ultraviolet and infrared radiation. Humidity and Moisture. Vol I, Principles and Methods of Measuring Humidity in Gases. Wexler, A. and R.E. Ruskin (Eds.), Reinhold Pub. Corp., New York, Ch. 43, 428-443.

Tricker, R.A.R., 1979: Ice crystal haloes. Atmospheric Optics Technical Group of the Optical Society of America, Washington, DC.

Turner, F.M., and L.F. Radke, 1973: The design and evaluation of an airborne optical ice particle counter. J. Appl. Meteor., 12, 1309-1318.

Vardiman, L., 1978: The generation of secondary ice particles in clouds by crystal-crystal collision. J. Atmos. Sci. 35, 2168-2180.

Varley, D.J., 1978a: Cirrus Particle Distribution Study, Part 1. AFGL-TR-78- 0192.

Varley, D.J., and D.M. Brooks, 1978: Cirrus Particle Distribution Study, Part 2. AFGL-TR-78-0248.

Varley, D.J., 1978b: Cirrus Particle Distribution Study, Part 3. AFGL-TR-78-0305.

Varley, D.J., and A.A. Barnes, 1979: Cirrus Particle Distribution Study, Part 4. AFGL-TR-0134.

Weickmann, H.K., 1947: Die Eisphase in der Atmosphere. Report and translations, 716, Ministry of Supply, London.

Wendling, P.R. and H.K. Weickmann, 1979: Scattering of solar radiation by hexagonal ice crystals. Appl. Opt., 18, 2663-2672.

Winn, W.P., 1968: Electrostatic theory for instruments which measure the radii of water drops by detecting a change in capacitance due to the presence of a drop. J. Appl. Met., 7, 929-937.

Yamashita, A., 1971: Skeleton ice crystals of non-hexagonal shape grown in free fall. J. Met. Soc. Japan, 49, 215-230.

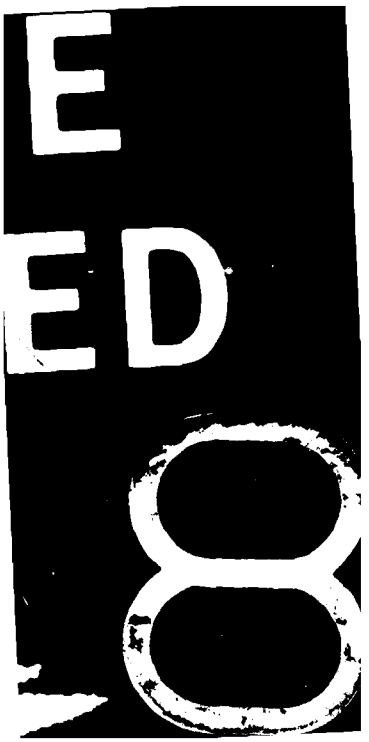
E
ED
8